

The role of inheritance in structuring hyperextended rift systems: some considerations based on observations and numerical modelling

G.Manatschal, L.Lavier and P. Chenin

Abstract

A long-standing question in Earth Sciences is related to the importance of inheritance in controlling tectonic processes. In contrast to physical processes that are generally applicable, assessing the role of inheritance suffers from two major problems: firstly, it is difficult to appraise without having insights into the history of a geological system; and secondly all inherited features are not reactivated during subsequent deformation phases. Therefore, the aim of this paper is to give some conceptual framework about how inheritance may control the architecture and evolution of hyperextended rift systems.

In this paper, we use the term inheritance to refer to the difference between an "ideal" layer-cake type lithosphere and a "real" lithosphere containing heterogeneities. The underlying philosophy of this work is that the evolution of hyperextended rift systems reflects the interplay between their inheritance (innate/"genetic code") and the physical processes at play (acquired/external factors). Thus, by observing the architecture and evolution of hyperextended rift systems and integrating the physical processes, one may get hints on what may have been the original inheritance of a system.

We first define 3 types of inheritance, namely structural, compositional and thermal inheritance and develop a simple and robust terminology able to describe and link observations made at different scales using geological, geophysical and modelling approaches. To this, we add definition of rift-induced processes, i.e. processes leading to compositional changes during rifting (e.g. serpentinization or decompression melting). Using this approach, we focus on 3 well-studied rift systems that are the Alpine Tethys, Pyrenean-Bay of Biscay and Iberia-Newfoundland rift systems. However, as all these examples are magma-poor, hyperextended rift systems that evolved over Variscan lithosphere the concepts developed in this paper cannot be applied universally. For the studied examples we can show that:

- 1) the inherited structures did not significantly control the location of breakup and the structures in the southern North Atlantic example
- 2) the inherited thermal state may control the mode and architecture of rift systems, in particular the architecture of the necking zone
- 3) the architecture of the necking zone may be influenced by the distribution and importance of ductile layers during decoupled deformation and is consequently controlled by the thermal structure and/or the inherited composition of the crust
- 4) conversely, the deformation in hyperextended domains is strongly controlled by weak hydrated minerals (e.g. clay, serpentinite) that result from the breakdown of feldspar and olivine due to fluid and reaction assisted deformation
- 5) inherited structures, in particular weaknesses, are important in controlling strain localization on a local scale and during early stages of rifting
- 6) inherited mantle composition and rift-related mantle processes may control the rheology of the mantle, the magmatic budget, the thermal structure and the localization of final rifting

These key observations show that both inheritance and rift-induced processes played a

50 significant role in the development of the magma-poor southern North Atlantic and
51 Alpine Tethys rift systems and that the role of inheritance may change as the physical
52 conditions vary during the evolving rifting and as rift-induced processes (serpentinization;
53 magma) become more important. Thus, it is not only important to determine the “genetic
54 code” of a rift system, but also to understand how it interacts and evolves during rifting.
55 Understand how far these new ideas and concepts derived from the well-studied
56 hyperextended rift systems of the southern North Atlantic and Alpine Tethys can be
57 translated to other less explored hyperextended rift systems will be one of the challenges
58 of the future research in rifted margins.

59
60
61

62 **1. Introduction**

63 Although there is general agreement in the community that inheritance has an important
64 influence on the architecture and tectonic evolution of rifted margins, it is not yet clear
65 how inheritance controls the initiation and evolution of rifting and lithospheric breakup.
66 Most studies advocating for a strong role of inheritance refer to the observed along strike
67 changes of the rift architecture and segmentation of rifted margins that seem to correlate
68 with changes in the onshore geology (Dunbar and Sawyer, 1989; Pique and Laville 1996;
69 Ring 1994; Tommasi and Vauchez, 2001). While Taylor et al. (2009) and Gerya (2012)
70 showed that major oceanic transform faults do not extend into the continents, Behn and
71 Lin (2000) discussed the importance of the segmentation observed along the U.S. East
72 coast passive margin for the incipient structure of the oceanic lithosphere. Thus, at present
73 it is not clear what is the importance of crustal inheritance in controlling the segmentation
74 in oceanic domains. Other studies discussed the reactivation of pre-existing faults, or
75 localization of deformation along major lithological boundaries (Butler et al. 2006;
76 (Bellahsen et al., 2012). These observations are most of the time local and are unable to
77 explain why early stages of rifting are often diffuse and do in most cases not coincide
78 with the location of final breakup (e.g. Dunbar and Sawyer 1989; Bertotti et al. 1993;
79 Manatschal and Bernoulli 1998). In the North Atlantic (Lundin and Doré, 2011) and the
80 NW Shelf of Australia (Direen et al. 2008), the final breakup cuts not only through
81 ancient orogenic belts, but also through earlier rift systems, suggesting that inheritance
82 does neither control the location of breakup, nor the onset of seafloor spreading.
83 Unfortunately, thick sedimentary and/or magmatic sequences prevent detailed
84 investigation of the pre-rift crustal and lithospheric structures and composition. Thus,
85 although the common belief is that inheritance has an important control on the evolution
86 of rift systems, at present it is difficult to assess under what conditions and how it controls
87 rifting and lithospheric breakup.

88 The aim of this paper is to define types of inheritance and to show, using
89 observations and models, how these different types of inheritance may control subsequent
90 rifting events. We use examples from the ancient and present-day Alpine Tethys,
91 Pyrenean-Bay of Biscay and Iberia-Newfoundland rifted margins to illustrate and discuss
92 ideas and concepts on how to integrate the role of inheritance in the study of rifted
93 margins. Since all rift systems discussed in this paper affect Variscan lithosphere and are
94 magma-poor, the ideas developed in this paper may not be applied globally. Thus, the aim
95 is not to propose models that can explain in a global way the influence of inheritance on
96 rift systems, but to discuss how “inheritance” can be described and integrated in
97 descriptions of hyperextended rift models leading to seafloor spreading.

98 Due to the very limited data from hyperextended rifted margins available in the
99 open domain and the difficulty to link their yet little understood evolution to inherited

100 orogenic structures, we will focus our paper on the well explored Variscan system in
101 Western Europe and its relation to the late rift evolution of the Alpine Tethys and
102 southern North Atlantic. Due to the novelty of the subject, this paper does not review but
103 does rather present some considerations on how inheritance may control hyperextended
104 rift systems based on observations and simple numerical models.
105

106 **2. Defining inheritance in rift systems and rifted margins**

107 Although the terms “inheritance” and “hyperextended rifted margins” are often
108 used, clear and universal definitions are necessary in order to discuss the impact of
109 inheritance on hyperextended rift systems. The aim of this chapter is to develop a
110 terminology that is simple, robust and that can describe and link observations made at
111 different scales using geological, geophysical and modelling approaches. The underlying
112 philosophy is that each rift system inherited a set of particular properties and boundary
113 conditions similar to a “genetic code”, and that the evolution of rift systems reflects the
114 interplay between their inheritance (innate) and the physical processes at play (acquired)
115 during rifting.
116

117 **2.1 Inheritance**

118 In contrast to oceanic domains that are newly formed and do, in theory, not bear
119 inheritance, continental domains are the result of polyphase tectonic, magmatic and
120 metamorphic events, often resulting from the superposition of several Wilson cycles.
121 Continental domains preserve a long history with a complex lithological and structural
122 record that cannot be described by few physical parameters only. Therefore, defining the
123 original state of the lithosphere at the onset of a new tectonic phase, in this case rifting, is
124 difficult. In this study, we use the term “inheritance” to refer to the difference between a
125 “real” and an “idealized” lithosphere (Fig. 1). The “idealized” lithosphere (Fig. 1a) is
126 defined as a thermally equilibrated horizontally homogeneous layer-cake lithosphere
127 made of a quartzo-feldspatic upper and middle crust and a mafic lower crust and a
128 peridotitic mantle (for definition of single layers see also (Sutra et al., 2013). In contrast
129 to this “idealized lithosphere”, a “real” lithosphere (Fig. 1b) may differ by its thermal
130 state, compositional heterogeneities and structural complexity.

131 We distinguish between three types of inheritance, namely “thermal”, “structural”
132 and “compositional” inheritance. Although the three can, practically, not be disassociated,
133 for simplicity we will discuss and exemplify the three independently. Figure 1b shows, in
134 a conceptualized manner, the 3 types of inheritance in a section across a lithosphere at the
135 end of an orogenic collapse but before onset of rifting. In this paper we only show
136 examples of rift systems that developed over Variscan post-orogenic, lithosphere. Other
137 types of lithospheres, not discussed in this paper, are cratonic or complex accreted
138 lithosphere, the latter formed by different terrains and separated by multiple suture zones
139 (e.g. Western North America).
140

141 **2.1.1 Thermal inheritance**

142 Two components have to be considered: 1) inherited heat and 2) potential of heat
143 production. Inherited heat decreases with time and is consequently a function of the age of
144 the lithosphere. This implies that the older the lithosphere, the colder the thermal structure
145 and the stronger the lithosphere. Thus, the time lag between the last thermal perturbation
146 of the lithosphere and the onset of rifting is of major importance in assessing the thermal
147 state of the lithosphere at the start of a rifting event. In contrast, the potential of heat
148 production depends on the presence of radiogenic elements, which is mainly controlled by
149 the composition and age of the crustal rocks and magmatic additions.

150
151
152
153
154
155
156
157
158
159
160
161
162
163
164
165
166
167
168
169
170
171
172
173
174
175
176
177
178
179
180
181
182
183
184
185
186
187
188
189
190
191
192
193
194
195
196
197
198
199

2.1.2 *Compositional inheritance*

Compositional inheritance can be defined as the difference between the real composition of a lithosphere relative to that of an idealized lithosphere made of layers with an homogeneous rheology (layer cake). Compositional variations may occur in the mantle as well as in the crust as a result of sedimentary, tectonic, magmatic, metamorphic and metasomatic processes during previous orogenic and extensional cycles. These compositional variations may be difficult to determine using seismic imaging methods alone and are often only determined by direct sampling of the lithosphere through xenoliths studies or sampling of remnants of former rift systems in orogens. As shown in Fig. 1b, in a post-orogenic crust, major compositional inheritances are remnants of flexural foreland basins and older post-orogenic intercontinental rift basins; ophiolite belts commonly associated with deep marine, clay/fluid rich thick sedimentary sequences, arc systems rich in new juvenile magmatic crust, and later orogenic underplated gabbroic bodies. In the mantle lithosphere, depletion and fertilisation of the lithospheric mantle are mainly related to subduction processes, slab breakoff, mantle plumes and post-orogenic extension. For instance, the mantle within a supra-subduction setting may be locally depleted or hydrated, while mantle rocks belonging to the down-going plate may not be significantly modified. The occurrence of underplated mafic bodies, often emplaced during slab breakoff or orogenic collapse can also result in the depletion of the underlying mantle. For cratonic lithosphere, long-term processes related to metasomatism and fertilization associated with magma-percolation may modify the composition of the lithosphere through time.

2.1.3 *Structural inheritance*

The existence of structures inherited from previous orogenic events in the crust and the underlying lithospheric mantle result in mechanical weak zones. These “weak” structures may correspond to ancient thrust belts or remnants of subduction zones. When these structures formed in the brittle layers, they are often linked to hydration processes. When they occur in the ductile layers, mainly as mylonitic shear zones characterized by grain size reduction and crystallographic preferred orientations, they can result in a strong anisotropy (Tommasi and Vauchez, 2001; Ring 1994). Of particular importance are intra-continental strike-slip systems, because these structures can affect the whole lithosphere (Tommasi and Vauchez, 2001), conversely to extensional or compressional structures, which are typically limited to the brittle lithosphere and become more diffuse in the ductile layers. It is also important to note that not every inherited structure has the potential to be reactivated. Reactivation depends on its orientation relative to the stress field, on its lateral continuity and on the rheological contrast of the encompassing rocks relative to the other lithospheric layers (e.g. Chenin and Beaumont, 2013).

2.2 *Hyperextended, magma-poor and polyphase rift systems*

The understanding of rift systems and rifted margins underwent a paradigm shift in the last two decades. This is mainly due to the development of new reflection and refraction imaging techniques at present-day deep water hyperextended rifted margins, deep-sea drilling along the Iberia/Newfoundland and East Greenland/Mid-Norwegian conjugate margins and studies of remnants of rift systems in collisional orogens (Peron-Pinvidic et al., 2013a). These studies resulted in new observations and interpretations of how rift systems evolve in time and space. This process enables us to describe the evolution of rifted margins and to classify them according to the following characteristics:

200 1) the volume and timing of magma formation during rifting (e.g. magma-poor vs.
201 magma-rich); 2) single vs. polyphase evolution (i.e. superposition of several rifting
202 events), and 3) the distribution and partitioning of deformation along strike (e.g.
203 segmentation associated with shear margins vs. orthogonal rifted margins).

204

205 *2.2.1 Magma poor vs. magma-rich rift systems*

206 Drilling of rifted margins by the Ocean Drilling Project (ODP) offshore Greenland
207 and Norway (ODP Legs 104 (Endholm et al. 1989), 152 (Larsen and Saunders 1998) and
208 163) Larsen et al. 1999), ODP Legs and Iberia and Newfoundland (ODP Leg 103 (Boillot
209 and Winterer, 1988), ODP Leg 149 (Whitmarsh and Sawyer, 1996), ODP Leg 173
210 (Whitmarsh and Wallace, 2001) and ODP Leg 210 (Tucholke and Sibuet, 2007) enabled
211 to distinguish between magma-rich and magma-poor rifted margins. While earlier models
212 suggested that these margins are end-member margins that evolved in a completely
213 different way, more recent studies suggest that they share many similarities and that both
214 evolve in a more similar way during early stages of rifting (Péron-Pinvidic et al. 2013).
215 Two processes seem to be common to all rifted margins: 1) tectonic thinning of the
216 crust/lithosphere and 2) lithospheric breakup induced magmatically/thermally (Fig. 2).
217 Many authors (Franke, 2013; Lundin and Doré, 2011; Peron-Pinvidic et al., 2013) (Keen
218 et al. 2012) suggest that magma-rich margins go through a phase of hyperextension pre-
219 dating the magmatic breakup (Fig. 2a). Thus, the major difference between magma-rich
220 and magma-poor rifted margins relates to their capacity to form large volumes of magma
221 over relatively short time frames at the time of breakup. Indeed, while at magma-poor
222 margins the time between onset of magma and lithospheric breakup can last over several
223 tens of millions of years (about 30Ma in the case of the Iberia margin), at magma rich
224 margins the timing between onset of magma formation and breakup is very short (<
225 5myr); see Fig. 2). In contrast to magma-rich margins, magma-poor margins offer two
226 major advantages in studying magmatic systems associated to rifting: 1) the final rift
227 structures are not masked by massive magmatic flows, and 2) exhumation of mantle rocks
228 offers the possibility to investigate the early stages of magma infiltration and its reaction
229 with deeper lithospheric levels.

230 In this paper, we focus on the examples of the magma-poor, hyperextended rift
231 systems of the southern North Atlantic and the Alpine Tethys since these are the only
232 ones whose hyperextended part benefits from either drill hole and high quality reflection
233 and refraction data or direct outcrop observation.

234

235 *2.2.2 Polyphase rifting*

236 Although the classical pure shear (McKenzie, 1978), simple shear (Wernicke,
237 1985) or the combination of the two (Lister et al., 1986) models are still largely used to
238 explain the evolution of rifted margins, the increased access to data and the development
239 of new dynamic models enable more accurate and observation-constrained scenarios for
240 the evolution of rifted margins. For instance, the dynamic model proposed by Lavier and
241 Manatschal (2006) builds on a large body of observations derived from the Alps and
242 Iberia. This model describes the evolution of rifting as a sequence of events referred to as
243 stretching, thinning, exhumation and seafloor spreading (see also (Péron-Pinvidic and
244 Manatschal, 2009) for a definition of these terms). In a more recent paper, (Sutra et al.,
245 2013) showed that mechanical coupling/decoupling of the crust and mantle during rifting
246 is reflected in the transition between thinning and exhumation. In this paper we mainly
247 use the terminology of these authors to describe the first-order evolution of rifting. All
248 these models have in common that rifting is, at first order, a strain localization process, i.e.
249 initiates over a wide area, localizes subsequently during necking and remains localized at

250 the mid-ocean ridge from breakup and onset of steady-state magmatic activity. However,
251 more and more evidence show that many rifts initially fail, migrate or step outside the
252 initial rift system before breakup occur resulting in so called “offset basins” (Chenin and
253 Beaumont, 2013). Here we call this phenomenon "polyphase rifting". Well documented
254 examples of polyphase rift include the NW Shelf offshore Australia (Direen et al. 2008),
255 the North Atlantic (Lundin and Doré, 2011), the northern segment of the South Atlantic
256 (Blaich et al., 2008) or the Southern-North Atlantic (Péron-Pinvidic and Manatschal,
257 2010). Why rift systems may fail or migrate and how far the localization/delocalization of
258 rift systems may be controlled by inheritance will be part of the discussion of this paper.
259

260 *2.2.3 Along strike variations, segmentation and 3D evolution of rift systems*

261 Most studies and models of rifted margins are focused on a 2D approach looking
262 at dip sections parallel to the kinematic transport direction. It is important to note that
263 these sections are not necessarily perpendicular to the margin, in particular in oblique or
264 shear margins. The along strike architecture of rifted margins characterized by
265 segmentation and strong lateral changes of crustal structures and/or the volume of
266 magmatic additions is not well understood. The hypothesis that inheritance and/or rift-
267 induced processes may control the lateral evolution and segmentation of rift systems is
268 discussed further below, based on the example of the southern North Atlantic.
269

270

271 **3. The role of Variscan inheritance in structuring the Alpine Tethys and Iberian rift-** 272 **systems**

273 Here we use the term “Variscan inheritance” to refer not only to the orogenic
274 processes but, also to the late to post-orogenic events, distinguishing between crustal and
275 mantle inheritance. We focus on the Alpine Tethys and Iberian Atlantic rift systems that
276 formed over a lithosphere with a strong Variscan inheritance. Although the fate of these
277 two conjugate margins are different, i.e. one became part of a big ocean while the other
278 probably never developed into a steady state ocean, we consider the two systems as
279 belonging to the same Late Triassic to Early Cretaceous rift system that formed over
280 Variscan orogenic lithosphere. Until now, most discussions of the importance of
281 inheritance focused either on local or large-scale examples, without considering that the
282 resolution of the observations is strongly scale-dependent. Here we try to integrate this
283 idea by discussing the role of structural and compositional inheritance at different scales,
284 ranging from lithospheric- to outcrop-scale.
285

286 *3.1 Influence of inheritance on a large-scale: the example of “Variscan” inheritance*

287

288 *3.1.1 Variscan processes controlling crustal inheritance*

289

290 *3.1.1.1 Pre- and syn-Variscan structures*

291 Akin to modern orogens, the Variscan orogen overprinted a continental
292 crust/lithosphere inherited from older orogenic events. The limit between parts of the
293 crust/lithosphere that were affected relative to those that remained unaffected by a severe
294 Variscan overprint corresponds to the transition between the fold and thrust belt and the
295 flexural foreland basin (Fig 3a and b). While this limit is well preserved across Northern
296 Germany and Southeastern England and Ireland, its southern limit is strongly overprinted
297 by the Mesozoic rifting and the Alpine orogeny (see Fig. 3). The main difference between
298 the distinct orogenic domains shown in Fig. 3a are, apart from their compositional and
299 structural inheritance, the age of the last tectonic/thermal event.

300 Capturing the details of the Variscan orogeny in Western Europe is at this stage
301 difficult, since the overall evolution and architecture is still a matter of debate (e.g.,
302 Martinez Catalan 2011). Indeed, remnants of the Variscan orogeny are dissected and
303 overprinted by later rifting and the Alpine orogenic cycle, which makes correlations
304 between the different parts of the former Variscan orogen difficult. The better-preserved
305 and continuous domain of the Variscan belt can be mapped through Eastern and North
306 Western Europe corresponds to the northern Variscan foreland and the associated fold and
307 thrust belt. More debated is the extent of the Rheic suture zone and that of arcs and back-
308 arc systems in Western Europe. This is mainly due to the poor preservation of this system
309 and the likely subduction of most material of the former internal parts, including the
310 remnants of the Rheic ocean and of the former arc and back-arc systems. Debated is also
311 the southern limit of the Variscan orogeny and the location of its associated foreland. The
312 occurrence of un-deformed Ordovician and Devonian sediments in the Southern Alps
313 suggests that the southern front coincides with the domain now occupied by the present-
314 day Alps (Raumer et al. 2012). However, possible late orogenic large-scale transtensional
315 or strike-slip systems may have dissected and displaced parts of the former orogen,
316 resulting in present-day juxtaposition of initially side by side terranes in a late stage of the
317 orogenic evolution (Raumer et al. 2012; Muttoni 2003). Another debate concerns the
318 relationships between the American and Iberian branches of the Variscan system. The
319 most popular interpretation is that the Variscan orogen formed an orocline (Pastor-Galan
320 et al. 2012), which is supported by the lack of Variscan overprint on the Newfoundland
321 margin. The drilling of Culm-type sediments, characteristic for the Variscan foreland, at
322 ODP Site 1069 along the deep Iberia margin supports this interpretation (for location see
323 Fig. 3a; (Wilson et al., 2001). Although details of the correlations and extent of the
324 Variscan range are not yet well constrained, at first order, the major paleogeographic
325 domains, including foreland basins, fold and thrust belts and internal parts (suture zone)
326 can be mapped on the scale of Western Europe. However, the lithospheric structure,
327 including the upper mantle and lower crust, have been strongly overprinted and modified
328 during the late to post-orogenic evolution of the orogeny as shown in the following
329 sections.

330

331 *3.1.1.2 Late- and post-Variscan structures*

332 Within the Variscan domain, the lithospheric and crustal structures are the result
333 of a complex evolution that ended with major late- to post-Variscan extensional and
334 magmatic events. Although the exact timing and processes of this evolution are not yet
335 well constrained on the scale of the whole orogen, it looks as if at about 310 to 300 Ma
336 the magmatic system changed from an arc-dominated to an intracontinental magmatic
337 setting. This change is associated with the emplacement of prominent underplated mafic
338 bodies and extrusive magmatic systems simultaneous with crustal thinning (Fig. 3c).
339 Evidence for magmatic underplating is widespread and can be observed in all exposed
340 sections preserving pre-rift lower crust (e.g. Ivrea zone in the Southern Alps (Peressini et
341 al. 2007), the Malenco-Campo-Grossina units in the Eastern Alps (Hansmann et al. 2001;
342 Tribuzio et al. 1999), the Santa Lucia complex (Rossi et al. 2006) and Calabria
343 (Caggianelli et al. 2012) as well as in xenoliths from the Variscan belt (e.g. xenoliths
344 from the French massif (Féménias et al. 2003)).

345 This event, also referred to as the “Permian event”, was concomitant with a
346 change in the morpho-tectonic evolution of the former orogenic system. It is expressed as
347 a shift from a classical mountain belt topography to one dominated by plateaus dissected
348 by intra-continental sedimentary basins (Burg et al. 1994; Froitzheim et al. 2008). This
349 evolution can be compared with the observed orogenic collapse in the Basin and Range

350 Province of the western US. The Permian Variscan collapse is not only recorded by the
351 important magmatic additions to the crust (intrusions and underplating), but also by
352 granulite facies metamorphism (Galli et al. 2011, see also Mohn et al. 2010 for a review),
353 which indicates a very high thermal gradient (Müntener et al. 2000, Schuster and Stüwe
354 2008). These authors described the thermal evolution during the late- to post-orogenic
355 event and determined the thermal state of the lithosphere at the end of Permian time, i.e.
356 before onset of rifting. These studies showed that the magmatic and thermal evolution
357 recorded in the continental crust is intimately related to processes acting in the underlying
358 mantle lithosphere (Fig. 3c). As discussed in the following, these processes strongly
359 controlled the final structure of the lithosphere at the end of the Variscan cycle and pre-
360 determined the conditions at the onset of the Mesozoic rifting.

361

362 *3.1.2 Variscan processes controlling mantle inheritance*

363 In most rift systems, the composition and evolution of the sub-continental mantle
364 involved in rifting is unknown and very difficult to either image or sample. Exceptions are
365 the Iberia-Newfoundland and the ancient rift systems/margins exposed in the Pyrenees
366 and the Alps. In these examples the mantle underneath the continent during rifting was
367 exhumed at the seafloor at the end of rifting. This exhumed mantle was drilled in the
368 Iberia margin and can directly be sampled in the Alps and Pyrenees. This offers the
369 unique opportunity to investigate the nature of subcontinental mantle and its evolution
370 during rifting and to explore the importance of inherited compositional variations.

371

372 *3.1.2.1 Pre- to syn-Variscan inheritance*

373 Mantle rocks drilled along the conjugate Iberia-Newfoundland margins (e.g. ODP
374 Sites 637 (Galicia Margin), 987, 899, 1068, 1070 (Iberia Abyssal Plain) and 1277
375 (Newfoundland) (see Fig. 4b) show distinct compositional heterogeneities (Fig. 4a;
376 Müntener and Manatschal, 2006) and references therein). While the mantle rocks from
377 the Newfoundland margin (ODP Site 1277) are made of depleted harzburgites (high
378 ratios of Cr# in clinopyroxene vs. spinel), those from the Iberia margin are less depleted
379 and consist of infiltrated plagioclase peridotites (Müntener and Manatschal, 2006). The
380 authors interpreted the strongly depleted harzburgites drilled at ODP Site 1277 at the
381 Newfoundland margin as derived from the hanging wall of a Caledonian subduction (Fig.
382 4b). Thus, these mantle rocks sampled the strongly depleted supra-subduction mantle that
383 may have produced the magma of the Bay of Island arc complex now exposed in
384 Newfoundland. This interpretation assumes that mantle rocks from the Ocean Continent
385 Transition (OCT) are derived from the pre-rift sub-continental mantle proving the
386 existence of a strong mantle inheritance. The observation that the mantle rocks from the
387 Iberia-Newfoundland margins show different degrees of depletion is a key observation,
388 because mantle composition is a key parameter controlling the magmatic volume that can
389 be produced during rifting.

390

391 *3.1.2.2 Post-Variscan to early rift inheritance*

392 In the Alps and Pyrenees, remnants of mantle rocks are common and associated
393 with lower to middle crustal granulites and deep marine sediments (Jammes, 2009;
394 Lagabrielle, 2009; Manatschal and Müntener, 2009) (Fig. 4d). Studies of these mantle
395 rocks in the Pyrenees (Lherz, LeRoux et al. 2007), Liguria and Corsica (Piccardo, 2003;
396 Rampone and Hofmann, 2012) (Montanini et al. 2012, and the Alps (Lanzo, Malenco,
397 Totalp; (Müntener et al., 2010) Piccardo et al. 2009,) showed that the mantle rocks
398 exhibited different degrees of modifications prior and during rifting. The uppermost
399 subcontinental mantle that locally still preserves primary contacts to the overlying crust

400 (e.g. Manlenco, Hermann et al. 1997) was too cold to either melt or react with magma
401 during the Permian orogenic collapse and subsequent rifting. This type of mantle, referred
402 to as inherited mantle, is exposed in the most proximal parts of the OCT where it is often
403 associated with remnants of the thinned continental crust (e.g. Malenco or Tasna;
404 Müntener et al. 2004, 2010) (Fig. 4d). In contrast, the mantle rocks occurring in the more
405 oceanward part of the OCT show a more complex evolution (Fig. 4d). Müntener et al.
406 (2004) showed that these mantle rocks record two major events: 1) a strong depletion
407 during the late- to post-orogenic event; and 2) an enrichment of the mantle during early
408 stages of rifting. The first event is dated as Permian by Sm/Nd model ages, interpreted to
409 date the melting of this mantle under asthenospheric conditions (Rampone and Hofmann,
410 2013; Müntener et al. 2004, 2010, and Piccardo et al. (2009). This event may be linked
411 with the emplacement of the gabbros shown in Fig. 3c at the base of the crust during
412 Permian time. The second event is associated with the infiltration and reaction of magma
413 with the previously depleted mantle. Thus, this second event has to be post-Permian but
414 pre-exhumation. These observations show that the subcontinental mantle records a
415 complex, polyphase evolution including depletion and fertilisation cycles. Thus, the
416 inherited subcontinental mantle underlying the domains that underwent rifting
417 experienced a strong late- to post-Variscan imprint. How this may have controlled the
418 subsequent rifting is discussed in the following section.

419

420 *3.1.3 Control of Variscan inheritance on the large-scale evolution of the Tethyan and* 421 *Iberian rift systems*

422

423 The extent of late Variscan overprint in the lower crust and mantle compared to pre-
424 and syn-orogenic compressional structures begs to the question of their relative influence
425 on the large-scale evolution of the subsequent rift system. In the following, we discuss the
426 role of the Variscan inheritance, in particular of lower crustal and mantle compositional
427 inheritance in controlling the large-scale strain distribution and magmatic evolution
428 during the subsequent rift event.

429 An interesting observation is that the location of hyperextension and later breakup
430 of the Alpine Tethys and Iberian Atlantic localized along the former boundaries of the
431 Variscan orogeny, leaving the central parts - thus all the previous suture zones - of the
432 orogenic lithosphere preserved (e.g. Bohemian massif, Massif Central and Armorican belt
433 and in the Iberian peninsula; Fig. 3a). This observation questions if the location of
434 continental necking and lithospheric breakup is pre-determined by orogenic or post-
435 orogenic processes.

436 How far gravitational processes, i.e slab breakoff and/or delamination of the
437 orogenic roots of an over-thickened orogenic crust are responsible for the subsequent rift
438 evolution compared to late- to post-Variscan inheritance is yet unclear. The observation
439 that in Western Europe crustal necking and breakup affected the boundaries between
440 internal and external parts of the former orogeny may suggest an “orogenic” control. One
441 factor that may control the location of necking is the late- to post-Variscan mafic
442 underplating, associated with the depletion of the underlying lithospheric mantle (Fig. 4c;
443 further discussion in section 5). Indeed, this process seems to be widespread but localized
444 underneath internal parts of the Variscan orogen (Fig. 3b). Thus, as shown by the
445 observations reported above, the Permian magmatic event strongly modified the crustal
446 and mantle composition underneath the realm affected by the Variscan orogen. This event
447 is well documented in all the geological sections that expose remnants of the Late
448 Variscan lower crust and mantle in the former distal portions of the Tethyan margin. It is
449 also drilled along the most distal Iberia margin (ODP Site 1967 in Fig. 4b), found in

450 xenolithes all over Western Europe (Féménias et al. 2003) and in remnants exhuming
451 lower crustal rocks in the Alps (e.g. Malenco; Herrmann et al. 1997). This suggests that
452 the last thermal event that may have modified in a severe way the lithosphere and modified
453 the composition of the lithospheric mantle and the lower crust is not related to the
454 Variscan collision, but the late- to post-orogenic extensional collapse of this orogen. In
455 the case of the Variscan orogeny, the post-orogenic collapse resulted in a stronger
456 lithosphere underneath previously overthickened crust comparing to the more external
457 and thinner crust in the former fold and thrust belt that was not modified (Fig. 3b).

458 A determinant observation for the magmatic evolution of the rifting event is that the
459 lithospheric mantle underneath Western Europe exhibits different degrees of
460 modifications prior and during rifting (Fig. 4a). The existence of depleted and enriched
461 mantle domains underneath crustal domains undergoing extension is important, since it
462 may explain differences in the magma production during rifting. Models assuming a
463 homogeneous subcontinental mantle explain the lack of syn-rift magma as either related
464 to very slow extension rates or a very cold mantle lithosphere or a combination of the two.
465 The depleted mantle domains that formed during the late to post-orogenic Permian event
466 may have lacked the necessary mineral components to produce melts during the
467 subsequent extensional event. It may explain why the rift system remained magma-poor.
468 Müntener et al. (2004) suggested, using the examples of the Alps that magmas first
469 reacted with the previously depleted lithospheric mantle before they were extracted
470 (Müntener et al., 2009). Assuming that these observations are generally valid, it would
471 mean that the subcontinental mantle was depleted during orogenic collapse and was
472 unable to produce a lot of magma during the following rifting. The first magma that was
473 formed by decompression reacted with the overlying depleted lithospheric mantle leading
474 to its fertilisation without any surface expression. This suggests that magma-poor rifted
475 margins may develop in the absence of plumes over a lithosphere that was depleted
476 during orogenic collapse. In contrast, magma-rich margins may occur over fertile mantle
477 lithosphere, either because it has never been depleted or because it was fertilized by a
478 plume or during previous rift-events. How important and how general these processes are,
479 is difficult to determine. However, it shows that linking β -factors to volume of produced
480 magma is an oversimplification and may not apply to domains where the subcontinental
481 mantle is heterogeneous.

482

483 ***3.2 Control of orogenic inheritance on a regional-scale: crustal necking and rifted*** 484 ***margin segmentation***

485

486 *3.2.1 Control of inheritance vs. rift-induced processes on the morphology of necking* 487 *profiles*

488 The Western Iberia margin is often considered as the archetype magma-poor
489 hyperextended rifted margin (Péron-Pinvidic et al. 2013). The numerous studies
490 performed along this rifted margin (e.g. (Tucholke et al., 2007), Péron-Pinvidic and
491 Manatschal, 2009) benefited from the dense covering of refraction and reflection seismic
492 and drill hole data. In particular the discovery of hyperextended continental crust begged
493 the questions of how the crust thins and what controls extreme crustal thinning? In order
494 to answer to these questions, Sutra and Manatschal (2012) defined and described necking
495 zones using reflection and refraction seismic lines from the Iberia rifted margin. These
496 necking zones correspond to areas where the crust is thinned from its initial thickness to a
497 crustal thickness of < 10km.

498

499 Observations

500 The architecture of the necking zone along the Western Iberia margin is shown in
501 three sections in Fig. 5a). The northern section corresponds to the ISE1 line (Iberia
502 Seismic Experiment; (Zelt et al., 2003), the central section to the composed LG12 - TGS
503 line (Sutra and Manatschal, 2012) and the southern section to the IAM 9 line (Dean et al.,
504 2000) (for location along the Iberia margin see Fig 3b). All sections are dip lines, i.e.
505 parallel to the kinematic transport direction. The necking domain has been defined as the
506 domain limiting original thick crust (30km) from crust thinner than 10km. The necking
507 zone is defined by an oceanward increase in the total β value, space accommodation and
508 the coupling of the deformation between crust and mantle (for a more detailed definition
509 of the “necking domain” see Sutra et al., 2013). In the northern section (ISE 1) the
510 necking profile is wide and defined by a double neck. In the central section (LG12-TGS)
511 the necking profile shows a single neck of intermediate width. In the southern section
512 (IAM 9) the necking is sharp. In contrast to the change of the necking profile along strike
513 of the margin, it is interesting to note that the width as well as the angle of aperture (angle
514 between top and base of the basement, the later corresponding to a “S” type reflection; e.g.
515 Sutra et al. 2013) of the coupled domain remains similar along the margin (Fig. 5a).

516

517 Implications

518 Thinning of the crust/lithosphere is one of the most fundamental processes related
519 to rifting. Extreme crustal thinning is typically localized within the so-called necking
520 domain, which can display strong lateral changes, as shown for the Iberian margin (Sutra
521 and Manatschal, 2012). The necking profile at rifted margins can be controlled by the
522 inherited bulk rheology of the crust, in particular by the relative distribution of ductile vs.
523 brittle layers (Mohn et al., 2012; see also discussion of modelling results in Section 4).
524 The observations show that the more ductile the crust, the more difficult it is to neck.
525 Conversely, strong and more rigid crust tends to produce sharper necks. Other controlling
526 parameters are the obliquity of extensional systems and the strain rate (Jammes et al.,
527 2010). For the example, the Iberian margin formed by orthogonal extension more than
528 100 myr after the last thermal imprint, suggesting that the lithosphere was thermally
529 equilibrated, and under similar strain rates along its whole length (see Sutra et al., 2013).
530 As the necking profiles are quite different along the margin, one can assume that their
531 architecture is primarily controlled by the composition of the crust and mantle. If we
532 assume a homogeneous mantle composition, the change in the necking profile observed
533 along the Iberia margin may provide some information about the inherited crustal
534 composition and indirectly about the bulk rheology of the crust at the onset of rifting. As
535 shown in Fig. 5b, the 3 sections cross different parts of the Variscan belt, which are likely
536 to show different crustal compositions (i.e. different percentages of ductile material and/or
537 inherited structures able to localize deformation). In the North (Fig. 5b), where the
538 necking profile is a wide double neck, the crustal structure is likely to be complex,
539 probably bearing several brittle-ductile transitions and/or strong lateral variations of the
540 crustal structure. In the South, where the necking profile is narrower, the crustal structure
541 is likely to be simpler, consisting of more brittle material and/or controlled by an
542 important inherited crustal scale structure (Alves, 2011).

543 Another important observation is that all sections shown in Fig. 5a display similar
544 width and angle of aperture of the coupled domain along strike (Fig. 5a). The map in Fig.
545 5c shows that the width of the coupled domain, which lies between the point of
546 exhumation and the coupling point (see Sutra et al., 2013 for details), does not change
547 along the margin, conversely to the width of the necking domain. Deformation in the
548 coupled domain only occurs via brittle processes, while it is primarily controlled by
549 ductile layers in the decoupled domain.

550 Based on the drilling results, the refraction velocities and in analogy with material
551 that can be found in comparable positions in the Alps, we assume that the crustal rocks
552 are strongly hydrated and that the bulk rheology of the hyperextended crust is mainly
553 controlled by the newly created phyllosilicates such as illite, chlorite and serpentinite. This
554 would explain that, when the crust is thinned to less than 10 km and becomes entirely
555 brittle, the initial compositional or structural differences do not impact deformation any
556 more and all crusts, independent of the initial composition, start to deform in a similar
557 way. Thus, while thinning and formation of the necking domain may be controlled, on a
558 crustal scale, by inheritance, deformation in the hyperextended and exhumation domains
559 is most likely not controlled by inheritance but by hydration processes, i.e. by a rift-
560 induced process. This applies, however, only to the uppermost parts of the hyperextended
561 crust and exhumed mantle (< 6km deep). On a lithospheric scale, the thinning of the
562 lithosphere and onset of magma may eventually control the localization of deformation
563 and magma-production controlling final breakup (see discussion section for more
564 discussion).

565 566 *3.2.2 Control of inheritance on the segmentation of rifted margins*

567 To what extent oceanic structures in general and transform faults in particular are
568 inherited from the previous rift system is highly debated (Bonatti et al., 1994). Taylor et al.
569 (2009) showed that oceanic transform faults do not penetrate into the margin, and (Gerya,
570 2012, 2013) showed that prominent structures observed on the continent do not necessary
571 continue into oceanic crust. However, at most present-day rifted margins the initial stages
572 associated with the development of highly segmented rift-transform margins are often
573 masked by thick sedimentary sequences and the relation between the rift structures, syn-
574 tectonic sediments and magmatic additions remain poorly constrained. A good place to
575 understand the role of inheritance on the segmentation of margins and hyperextended
576 domains, as well as the location of breakup and structures within the oceanic crust is the
577 Iberia Atlantic and Bay of Biscay – Pyrenean domain (Fig. 6). Welford et al. (2012) and
578 Tugend et al. (2014) showed that in these domains deformation was distributed over tens
579 of millions of years before it resulted in the opening of a spreading ocean that propagated
580 into a hyperextended and strongly segmented rift-transform system during Late Jurassic to
581 Mid Cretaceous time.

582 583 Observation

584 Alves (2011) showed that major lineaments observed and mapped onshore Iberia
585 can be observed and followed on potential field maps into the Zone of Exhumed
586 Continental Mantle (ZECM). This observation supports not only the idea that the mantle
587 is of subcontinental origin in the ZECM (see previous chapter), but also that these
588 structures are rooted into the lithospheric mantle. However, these lineaments disappear
589 further oceanwards as indicated by the observation that the magnetic anomaly 34 is
590 continuous and not affected by transfer faults along the Iberia-Newfoundland margins
591 (Fig. 6a). Thus, in this case, the structures observed in the continent do not control the
592 segmentation in the adjacent oceanic crust. Furthermore, none of the major transfer
593 structures along the southern North Atlantic, with the exception of the Torre Madeira –
594 Nova Scotia and Charlie Gibbs fracture zones seem to penetrate into the hyperextended
595 domains. This also suggests that inherited continental structures are unlikely to control the
596 structure of the adjacent oceanic crust.

597 Mapping of rift domains in the Bay of Biscay – Pyrenean system enabled the
598 description of inherited pre- and syn-rift structures and their relationships to the first
599 oceanic crust. Jammes, (2009) and Jammes et al. (2010b) showed that a network of

600 inherited structures such as the Toulouse and Pamplona faults localized and segmented
601 hyperextended rift basins. According to potential field maps, both the Toulouse and
602 Pamplona faults root deeply in the crust/lithosphere (Jammes et al. 2010b). A detailed
603 map of the rift domains (Tugend et al. 14) (Fig. 6b) shows the complex relationships
604 between the inherited Variscan and Late- to post-Variscan structures and the evolution of
605 the rift domain in space and time. On the large-scale maps (Fig. 6a) as well as on a
606 smaller-scale one inherited structures in the continent seem not to control the structures in
607 the adjacent ocean. This is well shown by the observation that the limit between the
608 hyperextended and oceanic domains remains unaffected by inherited structures mapped in
609 the continent. However, Tugend et al. (2014) and Jammes et al. (2010b) showed that
610 structuration of the hyperextended domain is strongly controlled by inheritance. Inherited
611 structures can either transfer extension (e.g. Pamplona fault), or control the polarity of
612 hyperextended margins, separating upper from lower plated margins (see Tugend et al.
613 2014).

614
615 Implications:

616 The observation that major structures observed in the continent can be prolonged
617 into the zone of exhumed mantle (e.g. Iberia Abyssal Plain; Alves, 2011) supports the
618 idea that the mantle underneath the OCT has a subcontinental origin. However, in the case
619 of the Iberian margin, these structures do not control the segmentation in the adjacent
620 oceanic crust. Furthermore, the major transfer structures in the oceanic crust along the
621 southern North Atlantic do not penetrate into the continent, suggesting that inherited
622 continental structures do not control the structure of the adjacent oceanic crust. The
623 observation that the first oceanic crust truncates earlier rift structures in the southern
624 North Atlantic (Fig. 6) suggests that breakup and seafloor spreading are not influenced by
625 inheritance but are the result of deep-seated asthenospheric processes. However, at
626 present the process of breakup is not yet sufficiently constrained to understand the
627 underlying controlling factors. The study of the Bay of Biscay – Pyrenean system shows
628 that stretching, thinning and exhumation are strongly controlled by inherited structures,
629 contrary to breakup and seafloor spreading. The latter may be controlled by heterogeneity
630 within the lithospheric mantle underlying the hyperextended domains (e.g. section 3.1.2).

631
632 **3.3 Control of inheritance on a local-scale**

633 In this section we use two examples to discuss how inherited structures and compositional
634 variations may control strain distribution on a local scale during hyperextension. The key
635 learning that we want to convey is the importance of inherited weak layers controlling
636 strain distribution and style of rifting. While the existence of pre-existing faults in the
637 brittle layer may be a common feature on rifted margins, the pre-rift salt example can be
638 used as an analogue for weaknesses such as weak layers in the crust or in the mantle able
639 to localize deformation.

640
641 *3.3.1 Relation between pre-rift structures and detachment faulting (Err detachment*
642 *system, SE Switzerland)*

643
644 General situation

645 The Err detachment system exposed in the Lower Austroalpine Err nappe in SE
646 Switzerland is one of the world's few exposed and preserved rift-related detachment
647 systems (e.g., Masini and Manatschal 2013). This structure can be mapped over about 200
648 km² exhibiting primary relationships with pre-rift Permian structures and Alpine thrust
649 faults. The Err detachment system formed during the final stage of rifting by sequential

650 faulting and exhumation. The detailed mapping of this rift related detachment system
651 (Froitzheim and Eberli, 1990; Manatschal and Nievergelt 1997; Masini et al. 2012) shows
652 the importance of the pre-rift structures for the localization of this long offset low-angle
653 extensional detachment structures.

654 655 Observations

656 The excellent exposure and preservation of the Err detachment system (Fig. 7a)
657 permit the determination of the relationships between inherited late Variscan (Permian)
658 structures and younger Alpine thrust faults (green and red structures in Fig. 7). Over wide
659 areas the Err detachment system corresponds to two well-defined, top-to-the-west
660 surfaces, referred to as the Err and the Jenatsch detachment faults (dark and light blue
661 structures in Fig. 7). These detachment surfaces are either overlain by extensional
662 allochthons, or, where the faults were directly exhumed at the seafloor, by syn-rift
663 sediments (Fig. 7c; see also Masini et al. 2012 for details).

664 A first observation establishes the relation between the detachment system and a
665 late Variscan batholith made mainly of granite. Throughout most of the observed area, the
666 granites form the footwall of the detachment system, while they are nearly absent in the
667 hanging wall. The primary intrusive contact between the host rocks and the granites, as
668 well as the occurrence of host rocks within the granites, can be observed in many places
669 in the footwall, suggesting that the detachment localized along, or near, the roof of the
670 batholith. A second key observation is the relationship between the detachment system
671 and a fault bounding a former Permian basin filled with a >500m thick volcano-
672 sedimentary sequence of Permian age and sealed by lower Triassic shallow marine
673 dolomites (Fig. 7b). As shown in Fig. 7c, the Jurassic detachment is overlain by the thick
674 Permo-Triassic succession in the area of Piz Surgonda. Directly to the North, the lower
675 Triassic dolomites are directly overlain, along a primary contact, by micaschists and
676 orthogneisses that are in the hanging wall of the Jurassic detachment (Fig. 7c). This
677 observation suggests that the Permian basin terminated abruptly north of the Surgonda
678 area along an East-West striking steep, south-dipping fault forming the northern
679 termination of the Permian basin (see Fig. 7d). Detailed mapping of the detachment
680 surfaces shows that the northern termination of the Permian basin corresponds to the
681 location where the Jurassic detachment fault system forms an East-West trending lateral
682 ramp. Thus, the lateral ramp of the detachment fault reactivates an inherited surface
683 corresponding to the northern termination of the Permian basin (see Fig. 7d). Mapping of
684 the major top-to-the-west Alpine thrust fault shows that it reactivates the Jurassic
685 detachment system in the south. In the north, where the Jurassic detachment fault forms a
686 lateral ramp, the Alpine thrust truncates this structure. This observation suggests that the
687 Alpine thrust was unable to reactivate the lateral ramp and incised into the footwall of the
688 Jurassic detachment. This can explain the observation that the Jurassic detachment system
689 was not reactivated during Alpine convergence and preserved its former relationship
690 between footwall and hanging wall in the vicinity of the lateral ramp.

691 692 Implications

693 The mapping of the well preserved Permian, Jurassic and Alpine structures in the
694 area of Piz Err – Piz Surgonda shows that the detachment faults localized either at
695 existing lithological contacts such as the limit between intrusive granites and the
696 surrounding host rocks, or that the detachment reactivated pre-existing structures. In the
697 example of Err detachment system, the complex 3D structure of the detachment system is
698 strongly controlled by the existence of a Permian basin as shown by the section that is
699 perpendicular to transport direction in Fig. 7c. These observations show that reactivation

700 of inherited structures or lithological boundaries with a major rheological contrast are
701 important and can control, on a local scale, the structures in hyperextended systems.

702

703

704 3.3.2 Relationships between pre-rift salt and detachment faulting (Mauléon and Parentis 705 basins)

706

707 General situation

708 The Mauléon and Parentis basins in the Western Pyrenees – Bay of Biscay formed
709 as hyperextended basins during Late Aptian to Albian time (Fig. 8a). Within these basins
710 salt structures have been drilled and are seismically imaged (e.g. Ibis glacier in Parentis
711 basin: Mathieu, (1986); Biteau et al. (2006)) and observed in the field (e.g. massif des
712 Arbailles, Roquiague diapir in Arzacq-Mauléon basin; Canérot (1989)) (Fig. 8b). These
713 basins offer therefore the opportunity to study the role of Triassic pre-rift evaporites
714 during the subsequent Late Aptian to Albian hyperextension using seismic and drill hole
715 data and field observations. Jammes et al. (2010a) and Lagabrielle et al. (2010) showed
716 that the pre-rift salt played an important role controlling the final structure of the
717 hyperextended basins. We consider the pre-rift salt as inherited compositional weaknesses,
718 similar to weaknesses in the crust and/or mantle, with the only difference that evaporites
719 are better exposed and their initial geometry better understood.

720

721 Observations

722 Within the Mauléon basin, the subsalt (basal Triassic Muschelkalk and Buntsandstein
723 units) and the supra-salt units (Upper Triassic to Lower Cretaceous carbonates) are never
724 juxtaposed within one continuous stratigraphic section. The sub-salt Lower Triassic
725 sediments (Buntsandstein and Muschelkalk) are associated with the Paleozoic meta-
726 sediments, while the supra-salt Upper Triassic to Lower Cretaceous carbonates form
727 massive tilted blocks, interpreted as extensional allochthons that overlay Triassic
728 evaporites and either continental or mantle rocks (e.g. Sarrance, Mail Arrouy blocks
729 (Jammes et al., 2009). Thus, in the Mauléon basin, the Triassic evaporites served as a
730 decoupling horizon separating sub-salt from supra-salt units. Although the present-day
731 position of these blocks is the result of Pyrenean compression, the occurrence of growth
732 structures of Early Aptian age (e.g. Urgonian carbonates in the Arbailles) indicates that
733 these blocks tilted during Early Cretaceous rifting using the Triassic evaporites as
734 decollement horizons. The observation of mantle rocks in salt diapirs within Upper
735 Cretaceous sediments show that salt had to be in direct contact with the exhumed mantle
736 already before Pyrenean convergence. An additional and independent argument is that a
737 hydrothermal metamorphic event, associated with mantle exhumation, and dated at 107+/-
738 3Ma, affected Triassic evaporites (Thiébaud et al., 1988, 1992). All these observations
739 show that there is a close relationship between salt, detachment faults and mantle
740 exhumation.

741

742 In the Parentis basin, diapiric structures occur mainly in the southern part (Mathieu,
743 1986; Biteau et al., 2006). Salt migration initiated in mid Cretaceous time and lasted until
744 the end of Eocene time. The relation between the salt and the rift structures can be
745 observed within a section running parallel to the coastline, referred to as the “Aquitaine
746 coast section” (Fig.8c). In this section, Jammes et al. (2010a) described along the southern
747 part of the section an extensional detachment structure that is related to salt migration.
748 Apart from the unmistakable evidence for salt diapirs (supported by drilling), there are
749 some hints for asymmetric blocks bounded by growth structures that are underlain by a

750 continuous, strong sub-salt reflector (Fig. 8c). The overall structure resembles that of
751 extensional allochthons. These structures look also similar to those observed in the
752 Arbailles, where tilted, fault-bounded blocks with Urgonian growth structures are
753 associated with salt diapirs (Canérot, 1989; see previous paragraph). About 2 km eastward
754 of the seismic section, two wells, SGM1 and CTS1, were drilled across the strong basal
755 reflector and penetrated into basement. Well SGM1 penetrated beneath Tertiary and
756 Upper Cretaceous sediments, 1737 m of Keuper salt series and 800 m of Triassic
757 Muschelkalk dolomite and Buntsandstein sandstones, and tectonized quartzite dated as
758 Carboniferous (Serrano et al., 2006). About 15 km to the north, located further basinward,
759 well CTS1 penetrates Tertiary and Upper Cretaceous sediments, 1189 m of salt, 500 m of
760 Lower Triassic sediments, and tectonized dolomites dated as Devonian (Serrano et al.,
761 2006). The large thickness of the salt series penetrated by these two wells supports the
762 presence of diapiric structures. The strong continuous reflector identified in the seismic
763 data corresponds to the top of the Triassic Muschelkalk dolomite, which lies at the base of
764 the Keuper salt. The continuity of this reflector under tilted blocks suggests that a
765 decollement occurs in the overlying salt series, an interpretation similar to that proposed
766 for the Mauléon area (see previous paragraph). The fact that the top of the basement is
767 tectonized shows that this deformation is not only due to gravitational deformation. A
768 major decollement located in the evaporitic Keuper is required to decouple deformation in
769 the supra-salt units from deformation in the sub-salt units. While the supra-salt
770 deformation was mainly accommodated by block tilting, the sub-salt deformation was
771 accommodated along a top basement detachment fault drilled at wells SGM1 and CTS1
772 (Fig. 8c). We propose therefore that the tilting of the Upper Triassic to Lower Cretaceous
773 carbonates, associated with the growth-structures (probably of Aptian age) occurred
774 simultaneously with, but decoupled from major crustal thinning in the underlying
775 continental crust (see model in Fig. 8d). The interaction of detachment faults and
776 decollements, the latter within the Keuper evaporites, can explain, as shown by Jammes et
777 al. (2010a), the unconformities observed and drilled in the southern Parentis and Mauléon
778 basins as well as the extreme thinning of the crust and local mantle exhumation observed
779 in these basins.

780

781 Implications:

782 The study of Triassic evaporite layers and their relationships to younger
783 extensional detachment faults exhuming deeper crustal and mantle rocks in the Parentis
784 and Mauléon basins enables us to suggest that the presence of a pre-rift salt layer in an
785 area undergoing extreme crustal thinning can control the geometry and evolution of rift
786 systems and obscure the rift related structures in the underlying basement. During an
787 initial stage of rifting, pre-rift salt layers act as a decoupling horizon between sub- and
788 supra-salt units suppressing the extension of the crustal detachment faults into layers
789 above the salt and, by doing so, eliminating breakaways at the seafloor (Fig. 8d). As a
790 consequence, the detachments sole out along the ductile salt layer and no sub-salt material
791 can be exhumed to the seafloor. Thus, sub- and supra-salt layers deform by different
792 deformation modes, which makes detachment faults difficult to identify on seismic
793 images. In a later stage, when salt has migrated and thinned out, sub- and supra-salt layers
794 can locally couple and detachment faults can daylight, resulting in the exhumation of
795 basement surrounded by extensional allochthons formed by supra-salt sedimentary units.
796 Thus, the pre-rift salt is a good illustration of the importance of inherited weak layers in
797 decoupling and localizing the deformation on a local scale during rifting. It may be seen
798 as an analogue for other potential weak layers in the crust or mantle, related to inherited
799 compositional inheritances.

800
801
802
803
804
805
806
807
808
809
810
811
812
813
814
815
816
817
818
819
820
821
822
823
824
825
826
827
828
829
830
831
832
833
834
835
836
837
838
839
840

4. Control of thermal state on the evolution of rifting: a modelling approach

4.1 Modelling approach

In his pioneering work, (Buck, 1991) showed that the thermal structure of the lithosphere is controlling, together with the composition and crustal thickness, the evolution of rift systems. Depending on the thermal structure and crustal thickness, Buck (1991) distinguished between “narrow”, “wide” or “core complex” extensional systems. Analogue models (Brun and Beslier, 1996) and numerical models (Huismans and Beaumont, 2007; Jammes et al., 2010) showed that, apart from the thermal structure and composition of the lithosphere, also the strain rate and obliquity may control the architecture of rift systems. The aim of this modeling study is to investigate the effect of the thermal structure on the dynamic behavior of the lithosphere during hyperextension. We consciously limit our models to very simple/basic to better investigate the very impact of different thermal structures. In contrast to compositional and structural inheritance, thermal inheritance is transient, therefore it would be difficult to investigate the effects of the thermal inheritance on hyperextension using fossil examples.

Following the work of Lavier and Manatschal (2006) we test the effects, on extensional styles and evolution, of variations in initial thermal structure in a rheologically layered lithosphere including a mafic (gabbroic) lower crust (Fig.9) assumed to be inherited from a phase of post orogenic collapse (see paragraph 3.1.1.2). The mantle is modelled as dry olivine and is assumed to be strong and depleted. We also include weakening of the crust by hydration where fault zones or ductile shear zone are active (for details see Fig. 9c) (Lavier and Manatschal, 2006). Finally, to limit the size of the parameter space we assume that the initial crustal thickness is dependent on the initial thermal structure. The numerical domain is initially 450 km wide and 100 km thick. (Fig. 9a). The crustal thickness is 35 km including a 7 km thick mafic layer at its base. Both numerical techniques and boundary conditions are identical to those used in Lavier and Manatschal (2006). To simulate rifting an extensional half rate of 2.5 mm/yr is applied on both side of the model (Fig. 9a). We vary the thermal structure assuming that the lithosphere cools rapidly after the phase of post-orogenic collapse. The lithospheric thickness is fixed to 100 km and we calculate an initial geotherm based on a fixed value of temperature at the Moho given by geological observation (i.e. Müntener et al. 2001). We define three cases: (1) the Moho temperature is set at 450°C for an old lithosphere (500 Myr) (Fig. 10), (2) 100 Myr later at 600°C (Fig. 11) and (3) immediately after post orogenic collapse at 750°C (Fig. 12). The first case could correspond to an ancient mobile belt and the intermediate case to the Tethyan rifting similar to what is observed in the Alps (for details see (Manatschal, 2004)). Even though these models are relatively simple when compared with the complex inheritances that could be ascribed (see previous sections), we obtain a wide range of tectonic behaviours and evolutions.

4.2 Modelling results

Figures 10, 11 and 12 show the results of the 3 different cases (1 to 3) with variable Moho temperatures. The figures show the evolution of the viscosity and strain rate over 30 Myr for each case (Fig. 10, 11 & 12). We distinguish 3 different styles of deformation: (see captions for details): (1) localized extension over a symmetric graben that roots in the mantle lithosphere that leads to rapid thinning and necking of the lithosphere until the mantle is exhumed at the surface (Fig. 10), (2) distributed extension followed by a phase of thinning during which necking of the lithosphere occurs for an intermediate lithosphere (Fig. 11), (3) highly distributed extension and near pure shear

850 deformation in case 1 with a hot/young lithosphere (Fig. 12). At first order the main
851 control on the different styles of extension is whether brittle deformation in the upper
852 crust is coupled to brittle deformation in the mafic lower crust and uppermost lithospheric
853 mantle. In case 3 the hot ductile lower crust allows for decoupling to be maintained over
854 very long time scales (30 myrs). In case 2 after being decoupled for ~ 13 Myr the middle
855 to lower crust eventually are thin enough that brittle upper crustal deformation can couple
856 to the deformation in the uppermost embrittled lithospheric mantle. At this moment in
857 time the lithosphere thins over a major lithospheric scale fault zone extending in the
858 mantle. In case 1 the lower crust and mantle lithosphere are mostly brittle and the
859 deformation is immediately coupled, leading to very localized rifts rooted in the mantle
860 lithosphere. The initial rapid subsidence of this keystone block, defined as block H in
861 Lavier and Manatschal (2006), is followed by rapid necking of the lithosphere and
862 extension and thinning of the internal parts of block H. Case 3 is an analogue of the
863 stretching phase and case 1 of the thinning phase defined by Lavier and Manatschal
864 (2006). Weakening of the crust by hydration (Lavier and Manatschal, 2006) develops
865 listric detachment faults that distribute the deformation in the upper crust. It also allows
866 for the formation of a weak middle crustal layer that decouples brittle deformation
867 between the upper and lower gabbroic crust. Finally the strong gabbroic lower crust
868 formed during the previous phase of extensional collapse act as a guide that distribute the
869 stress elastically or viscoelastically across the whole extensional domain. It becomes a
870 stress concentrator when brittle deformation can localize and propagate through it by
871 plastic (Mohr Coulomb yield) weakening as a function of plastic strain. Figure 13 shows
872 the state of the lithosphere and its topography after 150 km of extension for each case. At
873 first order case 1 develops a narrower conjugate margins with a large zone of exhumed
874 continental mantle. Case 3 develops upper-lower plate asymmetric conjugate margins in
875 a wider rift but a narrow zone of final thinning. This model does not reach exhumation
876 after 150km of extension. Case 2 is similar to that described in Lavier and Manatschal
877 (2006). The extension has stretched the lithosphere down to 20 km thickness (stretching
878 phase) before thinning it down to 10 km during the thinning phase preceding the
879 exhumation phase that brings some serpentinized mantle to the surface along a rolling-
880 hinge exhumation fault.

881

882

883

4.3 Implications

884

885

886

887

888

889

890

891

892

893

894

895

896

897

898

899

These models confirm that the thermal structure is a key parameter in controlling the rift evolution (Buck, 1991). The results of the models shown in Figures 10, 11 and 12 also emphasize the importance of the thermal structure controlling the necking architecture of the rifted margin. For higher temperature, a larger fraction of the upper lithospheric mantle and the continental crust are ductile. This results in the delocalization of the deformation and makes it hard to develop an area of necking where thinning of the crust and mantle are coupled and Moho-topography develops (Fig 12). In contrast, thinning of the crust and mantle are easily coupled and form sharper necks in colder settings (Fig 10). Thus, the evolution of a rift system depends on the thermal structure of the lithosphere in addition to its composition, rates and obliquity. For the same crustal thickness or tectonic province, young and hot lithosphere may be difficult to thin resulting in wide necking profiles, while old and cold lithosphere (Archean or Paleoproterozoic) may be strong, resulting in narrow necking profiles. The Variscan lithosphere underlying the Alpine Tethys and Iberia Atlantic margins follows a phase of Permian orogenic collapse that introduces a large amount of heat by magmatic processes and lithospheric thinning about 70 myr before onset of rifting. It may still be quite hot and may represent

900 an intermediate case between very young and very old lithosphere. Of course, these ideas
901 do neither consider compositional variations, nor strain rate, which may strongly modify
902 the bulk rheology of the extending lithosphere (see paragraph 3.2.1 and Fig. 5). At the
903 moment, we do not see how we can overcome the problem of constraining complex
904 structural and compositional inheritance, since we are not yet able to place realistic
905 “structural” or “compositional” inheritances in model and allow them to compete with the
906 thermal one. However, already taking into account variations in the thermal structure may
907 explain why most rift systems, except for those that are related to subductions (e.g. back-
908 arc situations; Tyrrhenian sea; Woodlark, Gulf of California), can not develop directly
909 from an orogenic collapse into a rift system (e.g. Basin and Range). It is likely that rift
910 systems cannot start within a crust/lithosphere that is too hot, probably because thinning
911 of the crust and the mantle cannot be coupled. In contrast, it may also be difficult to
912 initiate a rift system in a very cold lithosphere. This may explain why many rift systems
913 try, in an early stage, to avoid these domains and may prefer weak orogenic lithosphere or
914 other types of weaknesses.

915

916 **5. Discussion**

917 ***5.1 Relative role of inheritance vs. rift-induced processes***

918 The integration of inheritance in rift models is a key to eventually be able to
919 predict and understand the evolution of rift systems. However, as compositional,
920 structural and thermal inheritances cannot be disassociated one from each other, it
921 remains at present difficult to link particular rift structures or their evolution directly to
922 one specific type of inheritance. Furthermore, existing structures or weaknesses are not
923 always entirely reactivated as exemplified by the relation between Jurassic extensional
924 detachment fault and Alpine thrust in the vicinity of the a lateral ramp in paragraph 3.3.1,
925 (Fig. 7). Reasons may be that the geometry of the pre-existing structures/weaknesses are
926 complex (e.g. listric faults, ramps etc.), limited in their lateral extend (e.g. confined
927 evaporite layers), their orientation was not favourable to be reactivated, or the inherited
928 weakness is located in a layer not stiff enough to concentrate the stress (e.g. Chenin and
929 Beaumont, 2013). Another important point is that inherited weaknesses can either interact
930 or not depending on their scale and location within the lithosphere. For instance, mantle
931 weaknesses are unlikely to control the location of deformation at the surface as long as
932 deformation in the upper crust is decoupled from the underlying mantle.

933

934 In order to introduce this complexity into the description of rift systems, it is
935 important to define types of inheritance and to think about how, when and at what scale
936 they may control the rift evolution or rift architecture. In the previous chapters we showed,
937 based on natural examples that:

938

- 939 • inherited structures, in particular weaknesses, are important in controlling strain
940 localization on a local scale (e.g. Err detachment and Mauléon-Parentis examples; Figs.
941 7 and 8)
- 942 • the necking zones may be influenced by the thickness and distribution of ductile layers
943 during decoupled deformation (e.g. Iberia example; Fig.5; thermal results Figs. 10, 11
944 and 12)
- 945 • conversely, the deformation in the uppermost parts of the crust and exhumed mantle in
946 hyperextended, coupled domains seems not to be controlled by inheritance, but by
947 newly formed weak materials (clay, serpentinite, ...)
- 948 • mantle composition and mantle processes occurring before and during rifting may
949 control the magmatic budget, the thermal structure and the localization of final rifting

950 (e.g. Alps, Pyrenees and Iberia examples; Fig. 4) in addition to the rheology of the
951 mantle

- 952 • inherited structures within the crust do not significantly control the location of breakup
- 953 and the structures in the oceanic crust (e.g. Bay of Biscay and Iberian Atlantic; Fig. 6)
- 954 • the inherited thermal structure controls the mode and architecture of rift systems, in
- 955 particular the necking architecture (e.g. modelling approach; Figs. 10, 11, 12)

956

957 These key observations enable us to introduce inheritance in the rift models proposed
958 to describe the evolution of rifted margins. However, it is important to distinguish
959 between inheritance, and rift-induced processes, both of which can control rifting.
960 Examples of rift-induced processes include formation of clay, serpentization or
961 decompression melting. It is also important to note that the role of inheritance may change
962 as the physical conditions vary during the evolving rifting and as rift-induced processes
963 become more important. Inherited mantle composition may become particularly important
964 when the thermal structure of rifting evolves and magma production becomes an
965 important factor.

966

967 ***5.2 The role of inheritance within an evolving rift system***

968

969 *Modes of rifting*

970 Lavier and Manatschal (2006) proposed a dynamic model for magma-poor rift
971 systems, for which they defined different modes of rifting depending on the deformation
972 process(es) at play. These modes are referred to as stretching, thinning and exhumation
973 (Fig. 14). As discussed by Bronner et al. (2011), breakup at magma-poor rift systems may
974 only occur if an excess magmatic event is able to break the strength of the lithosphere and
975 to trigger steady state seafloor spreading. In order to capture the breakup process, we
976 define a "magmatic mode" pre-dating the "seafloor-spreading mode" (onset of steady-
977 state seafloor spreading).

978 Independently of their inheritance, margins may go through a sequence of
979 stretching, thinning, exhumation (not mandatory) and magmatic breakup. Although these
980 modes have been defined for the Iberia-Newfoundland and Alpine Tethyan margins
981 (Sutra et al. 2013, Mohn et al. 2013), they can be also recognized in most of the world
982 rifted margins, their importance and expression may change depending on the inheritance.
983 Therefore understanding which mode is controlled by what type of inheritance is a key to
984 describe and predict the evolution of rift systems (Fig. 14).

985

986 *Stretching mode*

987 During the stretching mode the total horizontal extension and the related crustal
988 and lithospheric thinning are minor, thus the thermal perturbation and the magmatic
989 production due to decompression melting are negligible. Therefore, in the absence of
990 magma (plume), the strength of the lithosphere is controlled by the strongest brittle layer,
991 which plays the role of a stress guider (see Lister and Davis. 1989). Brittle deformation is
992 decoupled along ductile crustal layers or ductile shear zones allowing brittle layers to
993 deform independently from each other. Thus, the evolution of rift basins in the stretching
994 mode is mainly controlled by inheritance/weaknesses in the uppermost brittle layer, which
995 is usually the upper crust. Inherited compositional weaknesses (pre-existing basins or
996 suture zones) or inherited structures (faults or shear zones) may control the localisation
997 during these initial stages of rifting. If magmatic activity occurs at this stage (often related
998 to plumes), magma can control the localization of deformation at this early stage of rifting
999 through thermal weakening (see East African rift).

1000

1001 Thinning mode

1002 Onset of the thinning mode corresponds to the failure of the brittle layers in the
1003 lithosphere and terminates with the attenuation of the last ductile layer (Pérez-Gussinyé
1004 and Reston, 2001). Thus, the location of necking may be controlled by weaknesses in the
1005 strongest brittle layer. For low to moderate thermal gradients this may correspond to the
1006 upper mantle (see deep necking depths of (Bassi et al., 1993). Thus, inheritance within the
1007 strong upper mantle may be important and control the location of the necking zone and
1008 ultimately the area of breakup. The necking process is mainly controlled by the capacity
1009 of the crust to decouple from the mantle lithosphere, i.e. the relative abundance of ductile
1010 crust over brittle crust, enabling to partition the deformation between the brittle and
1011 ductile layers. In contrast to the stretching mode where deformation is mainly limited to
1012 the crust, deformation is localized at a lithospheric scale during the thinning mode. How
1013 deformation is partitioned, how much pure-shear thinning occurs in the ductile layers and
1014 what processes really control the thinning of the crust are still a matter of debate. At this
1015 stage of rifting, it is very important to understand how brittle and ductile layers are
1016 distributed within the crust and lithosphere. Compositional and structural inheritance may
1017 control onset of thinning, while magma and fluids may become more important during the
1018 subsequent hyperextension. Therefore knowing the bulk rheological structure of the crust
1019 is essential. This may either be controlled by weak phases (hydrated phases, quartz rich
1020 rocks or metasediments in the crust) or strong phases (mafic bodies or granulites). The
1021 underthrusting or accretion of sediments during subduction or the existence of multiple
1022 sutures during accretion may create strong inherited weaknesses that may control the
1023 crustal thinning process. In systems with either high geothermal gradients or high
1024 percentages of ductile layers coupling may never be accomplished and Moho topography
1025 remains subdued despite of high amounts of extension (e.g. Basin and Range Province;
1026 Fig. 10). The overall thermal state is mainly controlling the brittle ductile transition. This
1027 becomes important because it ultimately controls the relative amount of ductile vs. brittle
1028 material in a crustal section. The colder the thermal state the more brittle the crust and
1029 lithospheric mantle and the faster coupling between crust and mantle will occur (Fig. 12).
1030 Conversely, the more ductile material the more extension is needed to reach the coupling
1031 point (see Figs. 10, 11 and 12 as well as Fig. 5).

1032

1033

1034 Exhumation mode

1035 During the exhumation mode, all the remaining continental crust is made of
1036 residual brittle layers, either upper crust, mafic lower crust, or former ductile crust that
1037 cooled and became brittle during thinning. At this stage, active brittle faults facilitate fluid
1038 transport and hydration of the crustal and mantle rocks, resulting in the serpentinization of
1039 the uppermost parts of the subcontinental mantle. Intense hydration modifies the original
1040 mineralogy controlling rifting (quartz, feldspar and olivine) to a new one controlled by
1041 clays and serpentine within the uppermost 6 kilometres of the basement. Thus, the
1042 rheology of the remaining crust is strongly controlled by weak, hydrated material.
1043 However, field observations show that, even during this late stage, local inheritance is
1044 important and the presence of inherited low-friction material (e.g. salt) or inherited
1045 structures may control the architecture of detachment systems on a local scale. However,
1046 on a larger scale it is not excluded that the newly formed weak material favours pure
1047 shear deformation to occur simultaneous to exhumation along localized detachment faults.
1048 Indeed, hydration of the crustal rocks (mainly feldspar to illite and chlorite) and mantle
1049 rocks (in particular olivine to serpentine) results in the formation of low friction mineral

1050 that may change in a significant way the rheology of the extending uppermost crust and
1051 exhumed mantle. It is important to note that these processes are a consequence of rifting
1052 rather than controlled by inheritance. This control by the change in mineralogy may be
1053 illustrated by the width of the hyperextended crustal wedge along the Iberian margin,
1054 which remains the same along the whole margin while the necking profiles vary strongly
1055 (e.g. Fig. 5c and discussion in chapter 3.2.1). This suggests that the processes controlling
1056 hyperextension and exhumation are different from those controlling necking. We assume
1057 that, within the coupled domain (< 10km thick), the material is formed by hydrated
1058 residual brittle parts of the continental crust, while further outboard, where the crust is
1059 thinned to less than 6km, it may overlie a serpentinized mantle behaving like a Mohr-
1060 Coulomb material with a low friction coefficient.

1061 Thus, the architecture of the hyperextended domain may be primarily controlled
1062 by newly formed clay, serpentine or talc resulting from hydration of the crust and/or
1063 mantle after their embrittlement, rather than by inheritance.

1064 1065 Magmatic mode

1066 Although magmatic activity may occur at low β (< 1.5) in rift systems, mostly as a
1067 consequence of magma input from a deep mantle source (e.g. East African and Rio
1068 Grande rifts), rift-related magmatism is usually a consequence of decompression melting
1069 related to extreme lithospheric thinning. The production of magma in rift settings is
1070 controlled by a number of processes and parameters, of which the thermal state, the rate
1071 of thinning, the shape of the base of the lithosphere, the content of hydrous phases in the
1072 lithospheric mantle and its composition. Composition and amount of water in the
1073 lithosphere (e.g. inherited depleted or fertile lithospheric mantle) are inherited and the
1074 thermal state allowing for magma formation is usually reached after the lithosphere has
1075 been thinned by at least 50%.

1076 In most rift models, mantle is considered to be homogenous and magma
1077 production controlled by strain (β). However, the study of mantle rocks derived from the
1078 Alpine Tethys and Iberia-Newfoundland rift systems showed that the continental
1079 lithosphere involved in rifting is strongly heterogeneous. Although it may be difficult to
1080 determine the composition and history of the subcontinental mantle rocks, observations
1081 tend to show that two processes are important in controlling the composition of the
1082 lithosphere, which are: 1) magmatic processes associated with former subduction zones
1083 (supra-subduction vs. subducted mantle); and 2) the post-orogenic thinning and melting
1084 (cleaning) of the mantle. It is interesting to note that the Variscan orogenic collapse
1085 resulted in strongly depleted subcontinental mantle in the Alps and in Iberia before the
1086 onset of rifting. This subcontinental mantle was subsequently fertilized by the melt
1087 produced during lithospheric thinning pre-dating lithospheric breakup. This "buffer
1088 effect" may explain the delay in the major magmatic pulse during rifting at these two
1089 magma-poor rifted margins. In this context it is also interesting to note that some of the
1090 classical volcanic rifted margins (magma-rich margins) may have initiated as magma-
1091 poor rift systems that underwent hyperextension prior to magmatic breakup. Examples are
1092 the North Atlantic Vøre and Møring margins or the NW Shelf off NW Australia (Péron-
1093 Pinvidic et al., 2013, Dieren et al., 2008). Indeed, at all these margins, the final magmatic
1094 breakup overprinted older hyperextended domains, suggesting that the breakup was not
1095 related to the previous extensional event, but triggered by the excess of magma. Similar
1096 observations can be made in other margins, where the final breakup crosscuts previous rift
1097 structures (see southern North Atlantic, Lundin and Doré, 2011). This begs the question
1098 of how much magmatic processes related to continental breakup are controlled by
1099

1100 inheritance? For example, for the Norwegian margin two possibilities can be envisaged:
1101 either the mantle was enriched as a consequence of earlier thinning (e.g. fertilisation of
1102 mantle during earlier rift events as discussed for the example of the Alps (Müntener et al.
1103 2004 and 2009), or it was triggered by the arrival of the plume, in which case no
1104 “inheritance” is needed to explain the magmatic breakup.

1105 This hypothesis suggests that the volume of magma generated during breakup is
1106 not necessarily a function of inheritance, but can be related to processes evolving in the
1107 underlying asthenosphere during hyperextension (e.g. Bronner et al. 2011). One of the
1108 reasons rift systems may fail, even after they went to mantle exhumation, is that they were
1109 not able to form enough magma to trigger the breakup (e.g. Porcupine, Rockall Trough,
1110 Orphan). This suggests that magmatic processes may represent the key control for
1111 continental breakup, being able to localize extension and force the lithosphere to break at
1112 any time. If this is true, lithospheric breakup is not controlled by extension or inheritance,
1113 but by asthenospheric (magmatic) processes.

1114
1115

1116 **Conclusion**

1117

1118 The key question that guided this study was to what extent inheritance may control
1119 the architecture, evolution and magmatic budget of hyperextended rifted margins. We
1120 defined 3 types of inheritance, namely structural, compositional and thermal inheritance
1121 and developed a simple and robust terminology able to describe and link observations
1122 made at different scales using geological, geophysical and modelling tools. Based on this
1123 approach, we focused on 3 well-studied examples that are the Alpine Tethys, Pyrenean-
1124 Bay of Biscay and Iberia-Newfoundland rift systems. Our work tends to show that, for the
1125 examples discussed in this paper:

- 1126 • inherited structures are important in controlling strain localization on a local scale and
1127 very early in the rift system.
- 1128 • shape of necking zones may be controlled by the occurrence of ductile layers within
1129 the crust, while necking efficiency may depend on stiffness of the necked layers
- 1130 • location of the necking zone may be controlled by the location where the strongest
1131 brittle layer may yield (in cold systems this may be the location where the upper
1132 lithospheric mantle starts to break).
- 1133 • deformation in the hyperextended and exhumation domains is primarily controlled by
1134 newly formed weak materials (clay, serpentinite, ...) that result from fluid circulation
1135 and reaction assisted deformation.
- 1136 • mantle composition and mantle processes occurring before and during rifting may
1137 control the rheology of the mantle, the magmatic budget, the thermal structure and the
1138 localization of deformation during late stages of continental crust attenuation and
1139 lithospheric breakup, while early stages are rather controlled by upper crustal inherited
1140 structures
- 1141 • inherited structures in the continental crust do not significantly control the location of
1142 breakup and the structures in the oceanic crust.
- 1143 • the inherited thermal structure controls the mode and architecture of rift systems, in
1144 particular the necking architecture

1145

1146 We conclude that both inheritance and rift-induced processes play a significant role in the
1147 development of rifted margins and need therefore to be introduced in the study of rift
1148 systems. However, as this study is exclusively based on the magma-poor Iberia-
1149 Newfoundland and Alpine Tethys hyperextended rift systems that developed over

1150 Variscan lithosphere, the applicability of our conclusions to other, less explored systems
1151 remains to be tested.

1152

1153

1154

1155 **ACKNOWLEDGMENTS**

1156 This manuscript benefited from the thoughtful and constructive reviews of Chris

1157 Beaumont and an anonymous reviewer. We thank Othmar Müntener, Garry Karner, Chris

1158 Johnson, Nick Kusznir, Gwenn Péron-Pinvidic, Suzon Jammes, Emmanuel Masini,

1159 Geoffroy Mohn, Julie Tugend and Emilie Sutra for helpful discussions. This research was

1160 indirectly financed and supported by several projects and companies (French Margins

1161 program; MM3 consortium, ExxonMobil, Total, Petrobras and the Agence Nationale de la

1162 Recherche (ANR)). A. Bouzeghaia is thanked for improving the quality of the figures.

1163

1164

1165

1166

1167

1168 **Figures**

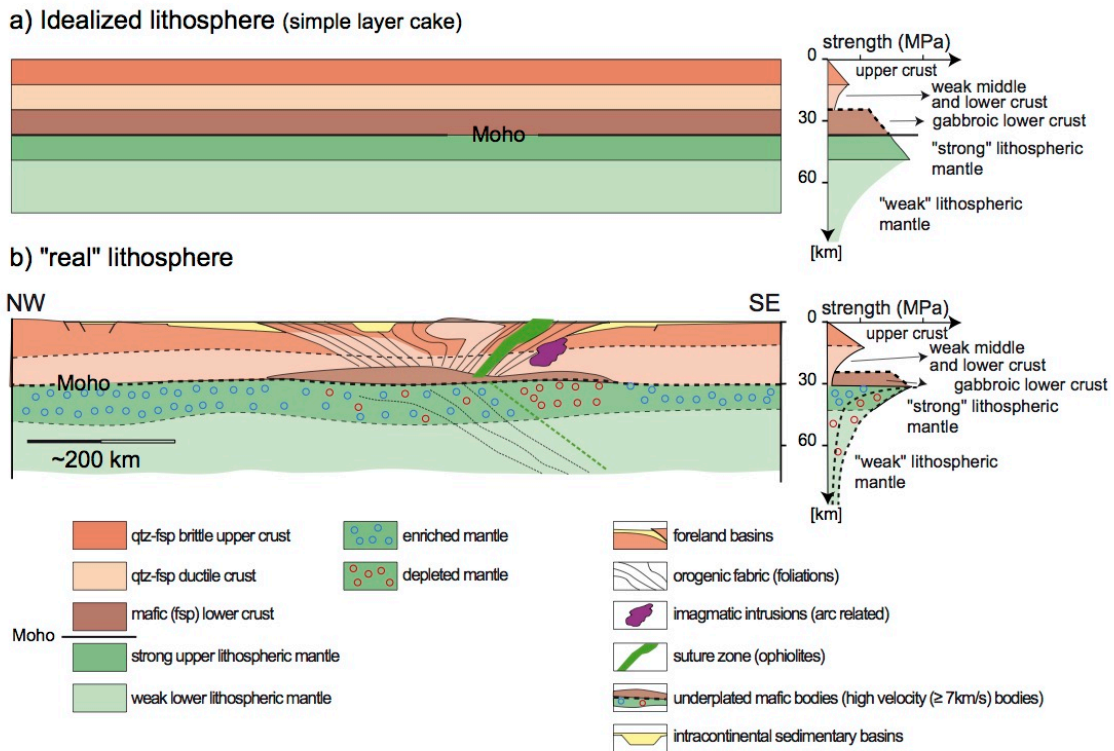


Fig. 1

1169
 1170 Fig. 1: Lithospheric scale sections showing (a) an idealized lithosphere made of a layer
 1171 cake and thermally equilibrated) and (b) a "real" post-orogenic lithosphere showing
 1172 inherited structural and compositional complexity.
 1173

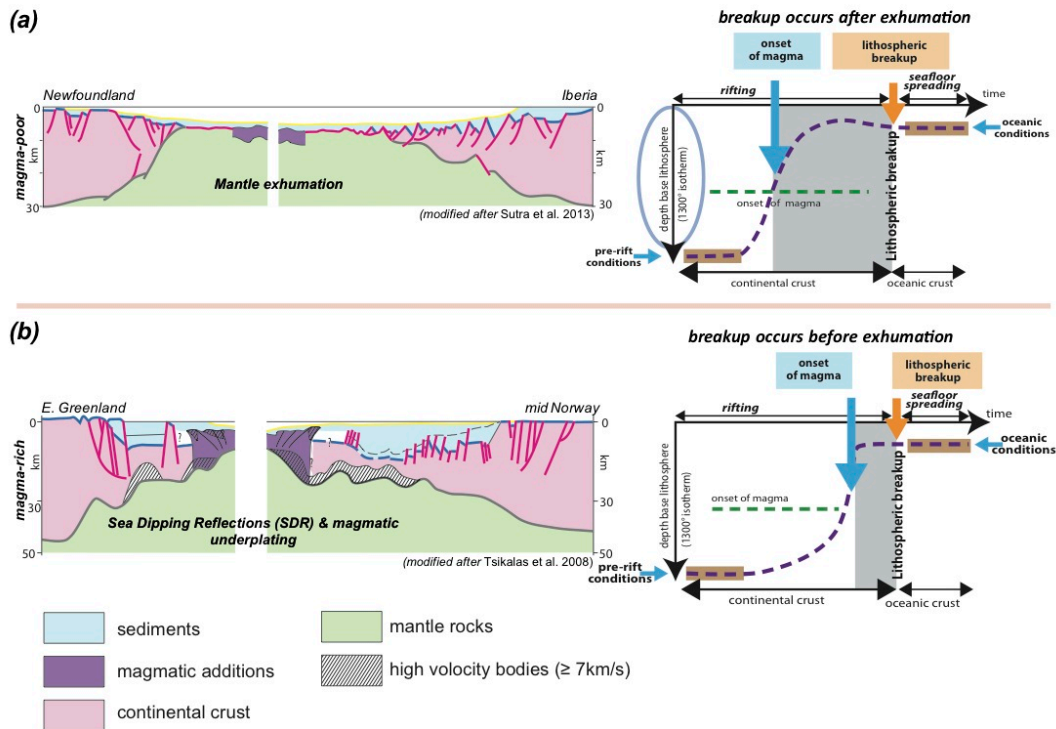


Fig. 2

1174
1175
1176
1177
1178
1179
1180
1181
1182
1183
1184
1185
1186
1187
1188

Fig. 2: Two sections showing (a) a magma-poor rifted margin and (b) a magma-rich rifted margin. The T-t evolution for a magma-rich margin and a magma poor margin is shown in a diagram where the vertical axis corresponds to the depth of the lithosphere (defined as the 1300°C isotherm) and the horizontal axis to the time axes showing the evolution of a system from rifting to seafloor spreading. The violet line shows the depth of the lithosphere as a function of time. The green line corresponds to the onset of magma-production that occurs when the lithosphere is thinned to < 50%. The grey domain corresponds to the time between first production of magma and the lithospheric breakup. Note that at magma-poor rifted margins breakup occurs after mantle has been exhumed, while at magma-rich rifted margins, breakup may occur before separation of the two continents.

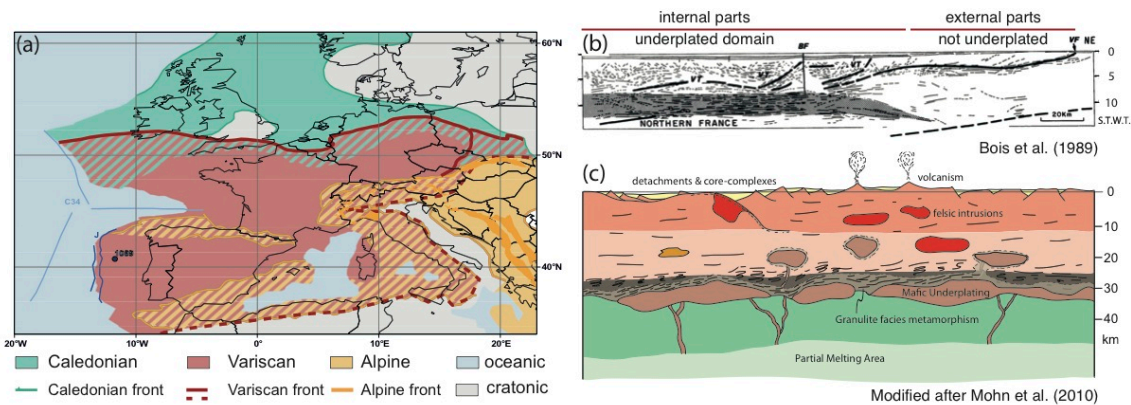


Fig. 3

1189 Fig. 3: (a) Map showing the nature of the lithosphere in Western Europe. Between
 1190 cratonic lithosphere in the northeast (Fenoscandia) and oceanic lithosphere in the
 1191 West (North Atlantic) and in the Mediterranean (back arc basins) the remainder of the crust
 1192 is either Caledonian, Variscan or Alpine (modified after Stojadinovic et al. 2013; Schmid
 1193 et al. 2004; Robertson et al. 2013; Cowie & Kusznir 2012, Barrier et al. 2004). (b)
 1194 Seismic section across the Northern Variscan domain in NE France showing the
 1195 occurrence of underplated mafic crust (high velocity reflective crust) underneath the
 1196 domain affected by the Variscan orogen. Note that the termination of the underplated
 1197 body coincides with the northern border of the Variscan orogen (from Bois et al. 1989).
 1198 (c) Schematic cross section showing the composition and major structures forming the
 1199 crust and upper lithosphere at the end of late Permian extensional collapse (modified after
 1200 Mohn et al. 2010). Note the occurrence of mafic (gabbroic) magmatic bodies at the base
 1201 of the crust as well as in mid crustal levels while the upper crust is formed predominantly
 1202 by felsic intrusions preferentially emplaced in upper crustal levels before 300Ma. In
 1203 contrast most mafic intrusions range between 300 and 250Ma. Note also the occurrence of
 1204 granulite facies contact metamorphism of Permian age that is associated with the
 1205 emplacement of the gabbros. The shallow position of the asthenosphere during the
 1206 Permian magmatic event results in high geothermal gradients and the depletion of the
 1207 mantle rocks (see text for explanations and references).
 1208
 1209

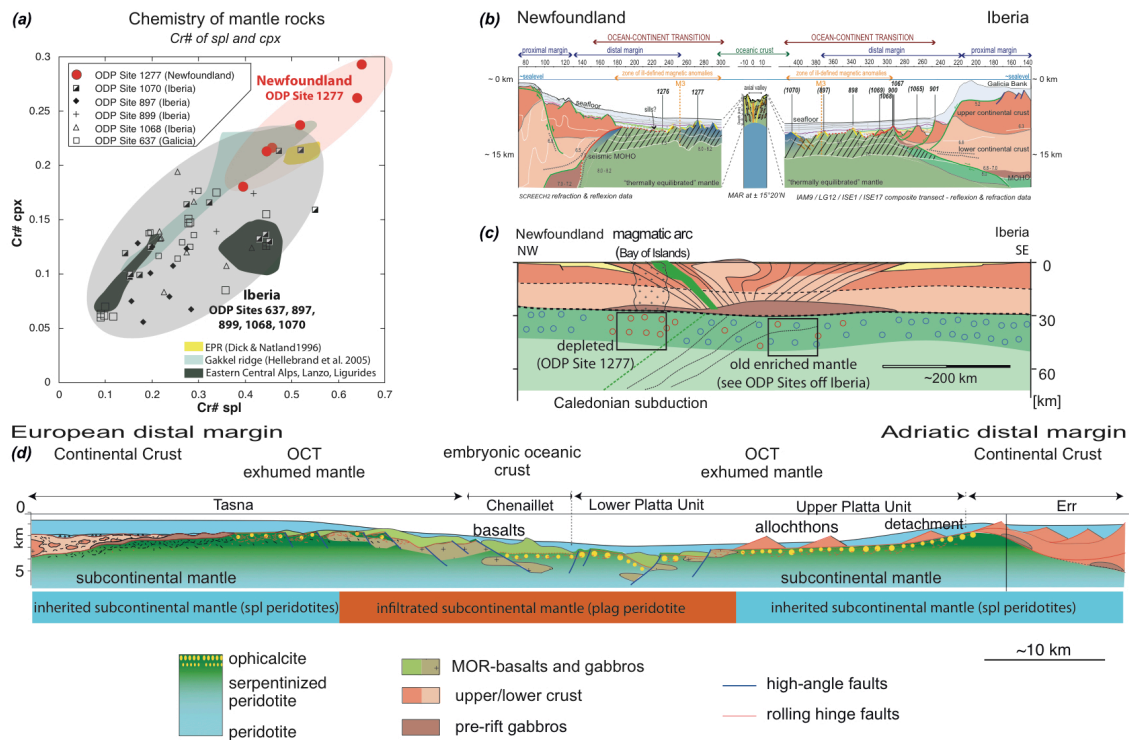


Fig. 4

1210
 1211 Fig. 4: Nature and composition of mantle rocks drilled along the Iberia-Newfoundland
 1212 rifted margins and exposed in the Alps. (a) Cr# of cpx versus Cr# of spinel in peridotites
 1213 from the Iberia–Newfoundland rifted margins. Light blue shaded field are spinel
 1214 peridotites from the Lena trough (Dick and Natland, 1996), dark grey shaded field are
 1215 spinel and plagioclase peridotites from the Eastern Central Alps (Müntener et al., 2004
 1216 and 2009), and the yellow shaded field is from the East Pacific Rise (Dick and Natland,
 1217 1996). Note that all samples from Site 1277 (Newfoundland margin) are aligned along the
 1218 Cr# covariation trend for spinel peridotites, while many samples from Iberia show
 1219 substantial deviation towards higher Cr# in spinel. This offset has been interpreted by
 1220 partial equilibration with plagioclase (for more details see Müntener and Manatschal,
 1221 2006). (b) Present-day section across the Iberia-Newfoundland rifted margin showing the
 1222 location of the drill samples (modified after Péron-Pinvidic and Manatschal, 2009).
 1223 Numbers refer to basement rocks drilled along the Iberia-Newfoundland margin. (c)
 1224 Simplified section across Iberia-Newfoundland showing the situation prior to onset of
 1225 rifting. Numbers refer to basement rocks drilled along the Iberia-Newfoundland margin;
 1226 for present-day position see section shown in Fig. 3b. (d) Distribution of subcontinental
 1227 inherited and infiltrated domains of mantle peridotite in the reconstructed OCT in the
 1228 Alps (modified after Manatschal and Müntener, 2009, and Müntener et al., 2009).
 1229

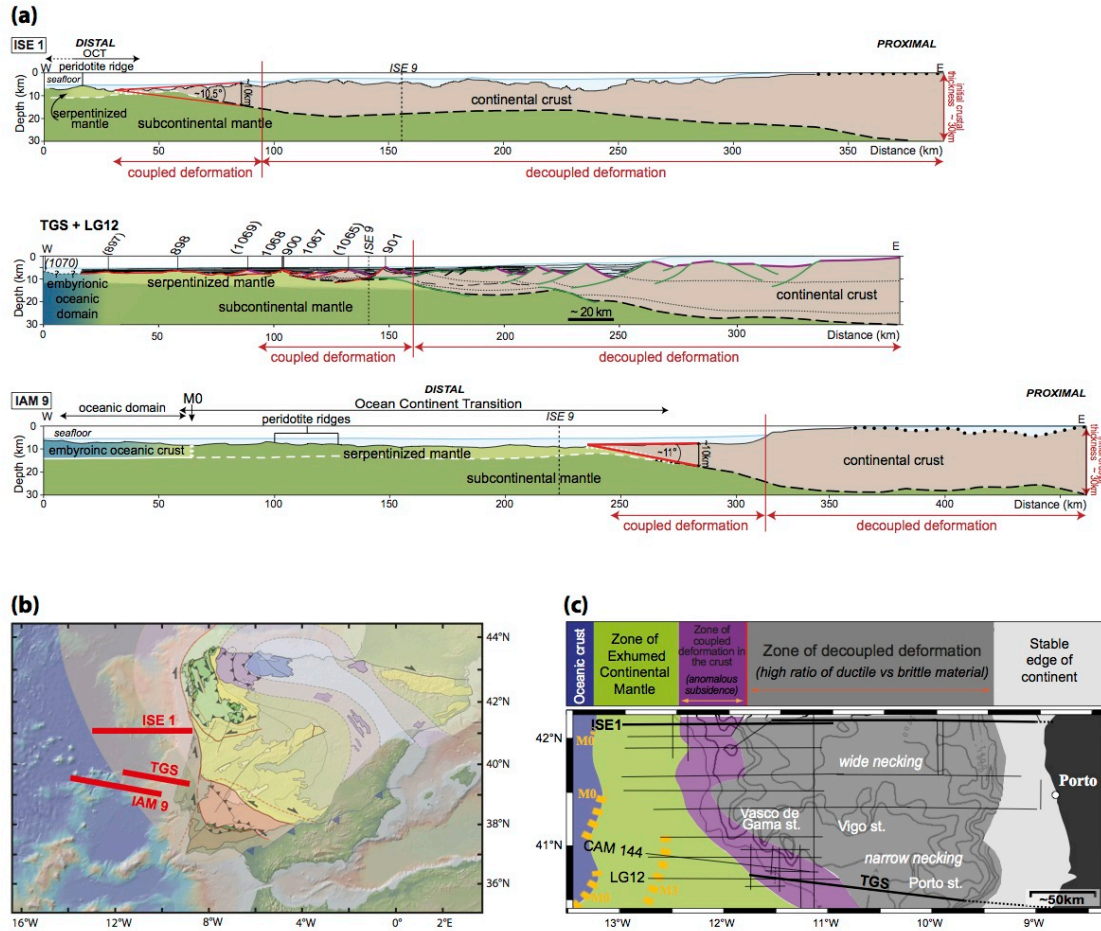


Fig. 5

1230
 1231
 1232
 1233
 1234
 1235
 1236
 1237
 1238
 1239
 1240
 1241
 1242
 1243

Fig. 5: Crustal architecture and necking profiles along the Iberia margin (a) Sections across the Iberia margin (for details see text, for location see Fig. 5b). The lines show the first order architecture of the continental crust, i.e. the change in crustal thickness across the margin. In the sections domains of decoupled thinning (e.g. necking zone), can be distinguished from a domain of coupled deformation (hyperextended crust) that lies between the coupling point and the point of exhumation (for details see Sutra et al., 2013). Angle of crustal wedge within the coupled domain is indicated in red. (b) Map showing the position of the lines shown in Fig. 5a. The map shows also the distribution of the crustal domains in Iberia compiled from Martínez-Catalán (2012), Ryan et al. (2009) and Higgins and Leslie (2000). (c) Map showing the distribution of decoupled deformation (necking domain) from coupled deformation (hyperextended domain) along the northwestern Iberia margin (modified after Sutra et al., 2012).

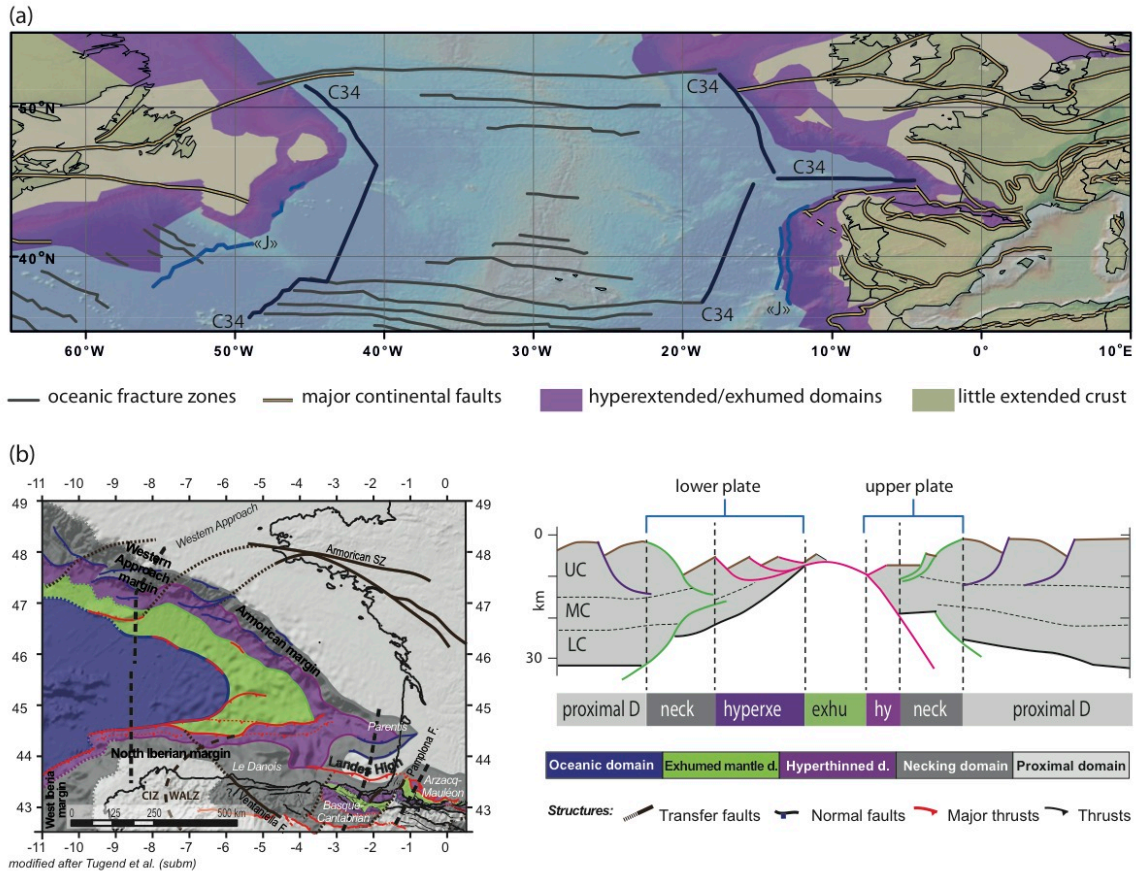


Fig. 6

1244
 1245
 1246
 1247
 1248
 1249
 1250
 1251
 1252
 1253

Fig. 6: (a) Map of the southern N-Atlantic showing the major structures such as oceanic fracture zones, OCT, necking zones, continental fracture zones and the magnetic anomalies 34 and J that are supposed to correspond to the continent ward limit of unequivocal oceanic crust and embryonic oceanic crust respectively. Maps compiled after Arenas et al. (2007), Ziegler and Dézes (2006), Mosar (2003) and Ryan et al. (2009). (b) Map of rift domains preserved in the Bay of Biscay and Western Pyrenees ; CIZ: Central Iberian zone. WALZ: West Asturian-Leonese zone. NPF: North Pyrenean fault (modified after Tugend et al. subm).

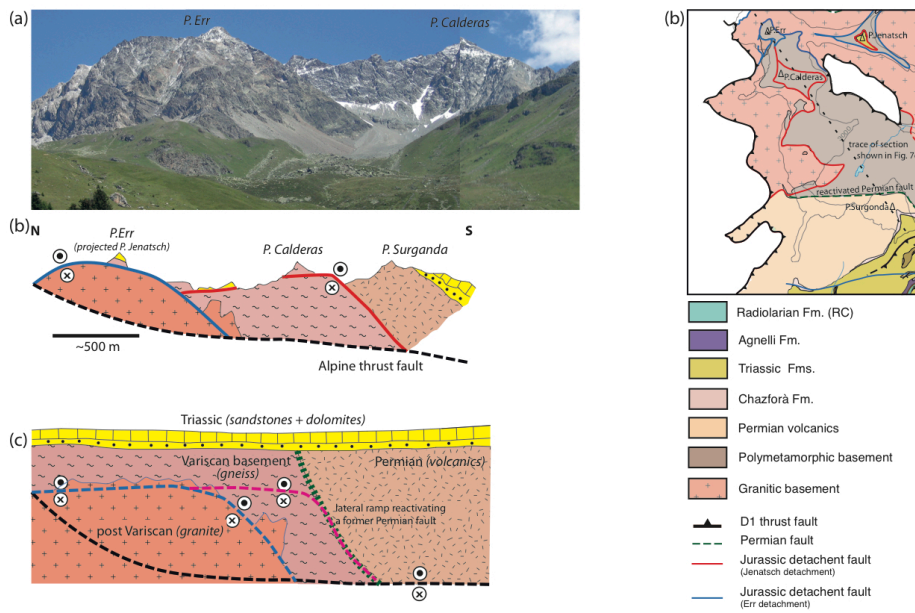


Fig. 7

1254
1255
1256
1257
1258
1259
1260
1261
1262
1263
1264

Fig. 7: (a) Panoramic view of the Jurassic extensional Err and Jenatsch detachment faults exposed in the Err nappe in SE Switzerland. View from west towards the East. (b) Map of the Err nappe in the area of Piz Err – Piz Surgonda, showing relations between the Jurassic extensional detachment system (in blue and red colours), a pre-existing Permian normal fault (in green colour) and an Alpine thrust fault (in black). (c) NW-SE cross section across the Err nappe showing the present-day relation between the Jurassic extensional detachment faults, the Permian fault and the Alpine D1 thrust fault. (d) A restored section showing the relationships before onset of Jurassic rifting and the traces of the future faults.

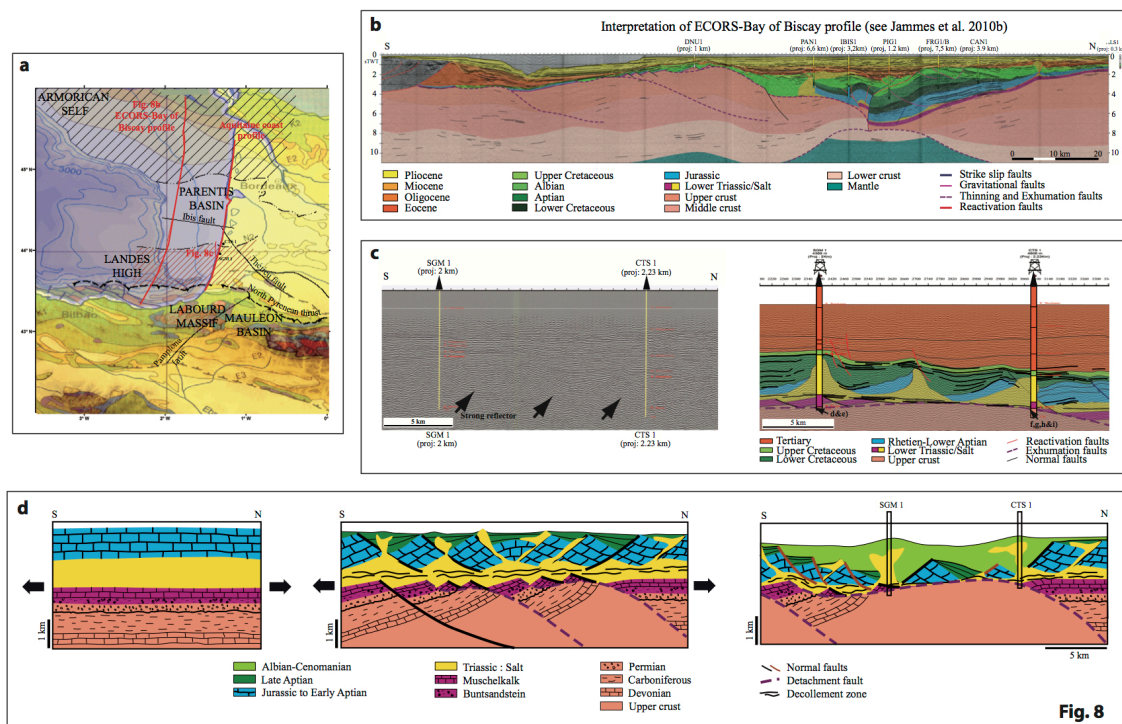
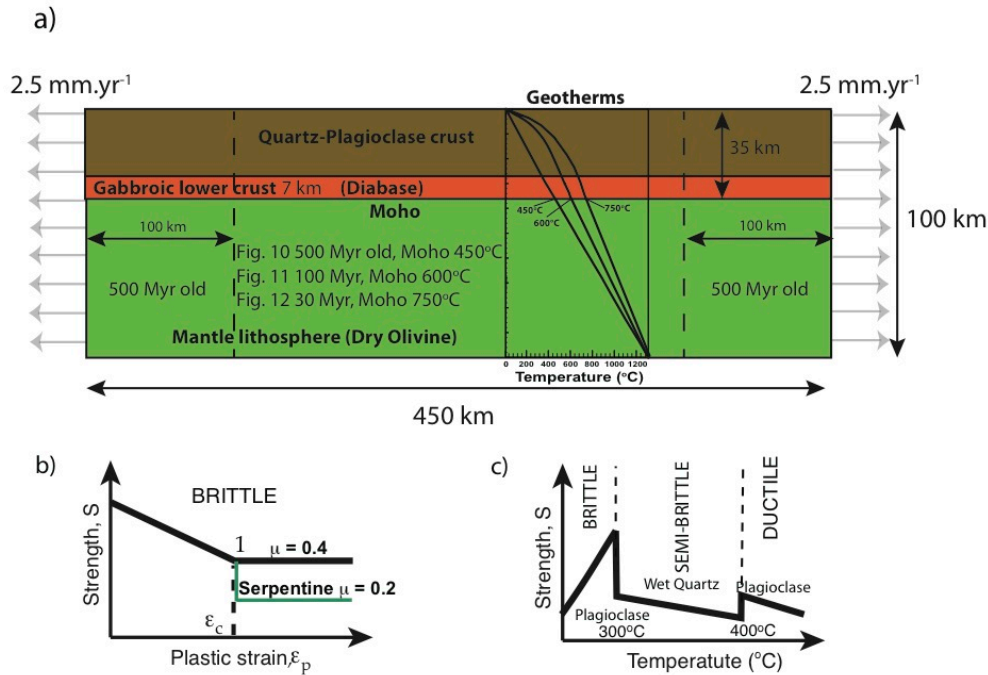


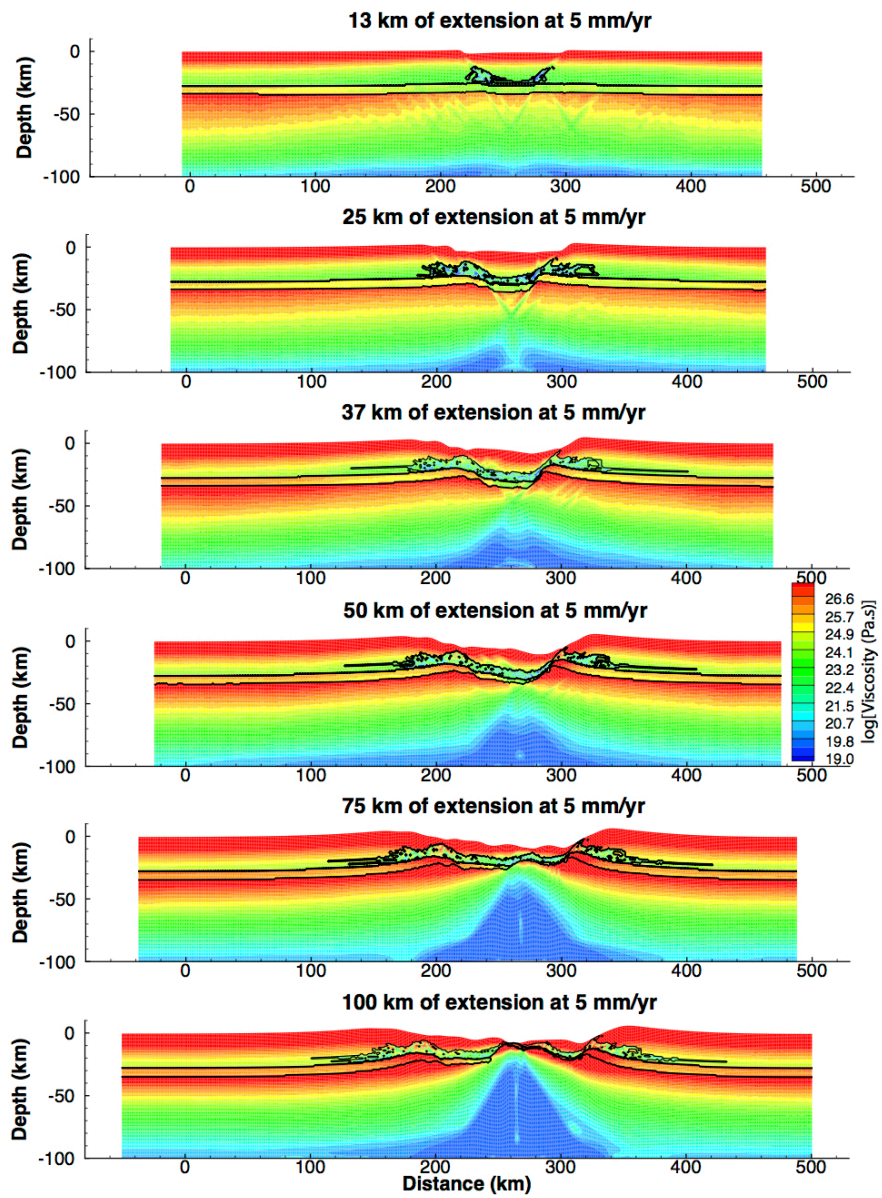
Fig. 8

1265
 1266 Fig. 8: Relationships between pre-rift salt and extensional detachment faults in the
 1267 Parentis and Mauléon hyperextended basins. (a) Map showing location of the Parentis and
 1268 Mauléon basins and location of seismic profiles shown in this figure. (b) ECORS-Bay of
 1269 Biscay profile with location of drill-holes. Interpretation taken from Jammes et al.
 1270 (2010b). CAN1 = Cormoran; FRG1/B = Frégate; PIG1 = Pingouin; PAN1 = Pélican;
 1271 IBIS2 = Ibis 2; DNU1 = Danu; ALS1 = Albatros; TWT = two-way traveltime. (c) Zoom
 1272 on the Aquitaine coast profile (modified after Jammes et al. 2010b). Note the presence of
 1273 the asymmetric blocks bounded by growth structures and soled by a strong reflection
 1274 indicated by black arrows. To the right, interpretation of the profile proposed by Jammes
 1275 et al. (2010b). Note also that drill holes penetrate deformed basement underneath the
 1276 Upper Triassic evaporate horizon. For more discussion see text. SGM1 and CTS1 = Saint
 1277 Girons en Marensin and Contis wells; line is in TWT (= two-way travel time). (d)
 1278 Conceptual model showing the function of the Triassic pre-salt during extreme crustal
 1279 thinning from the pre-rift stage to the stretching stage to the thinning stage. Note the
 1280 decoupling between the detachment faults responsible for crustal thinning and the pure
 1281 shear deformation within the Upper Triassic to Jurassic limestones. For location of wells
 1282 SGM1 and CTS1 see Fig. 8c and for details Jammes et al. (2010b).
 1283

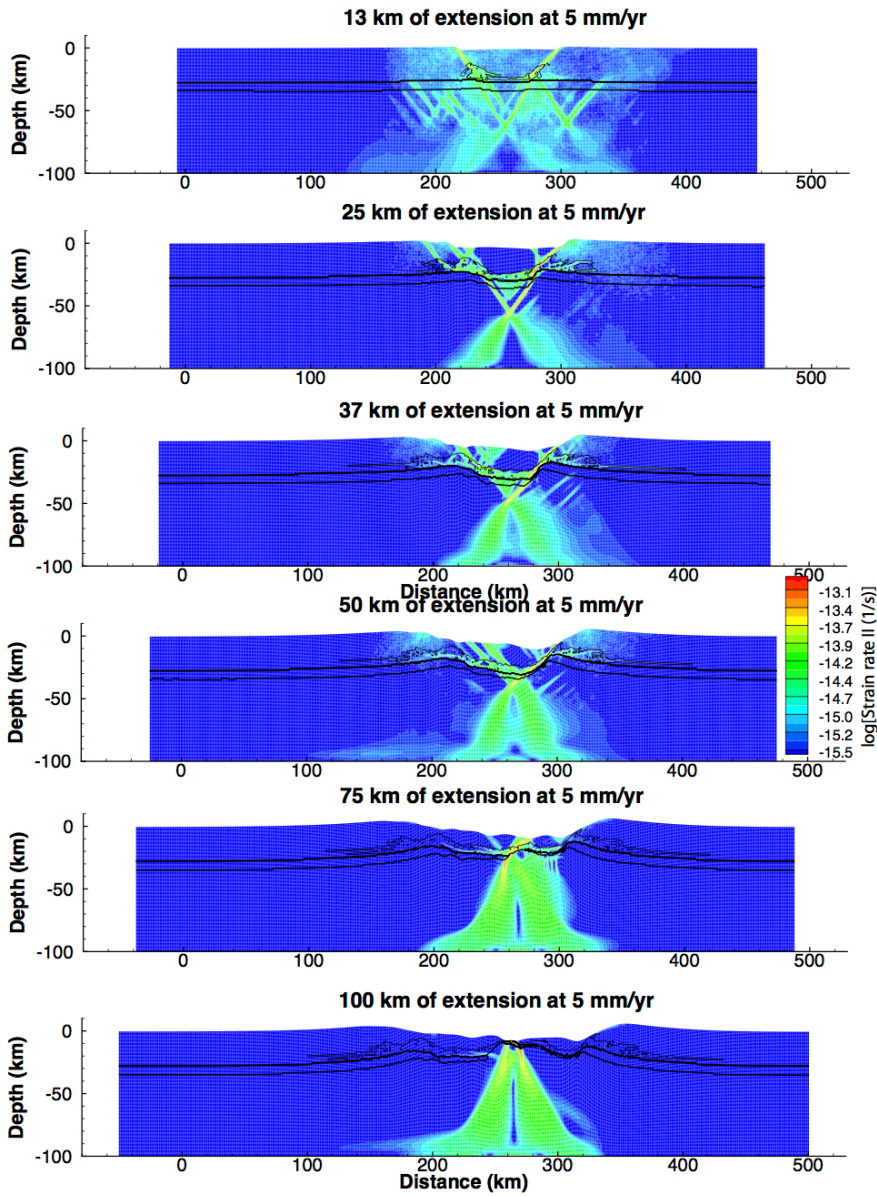


1284
 1285 Fig. 9: (a) The sides of the model are pulled apart at a constant half-rate of 2.5 mmyr⁻¹.
 1286 Isostatic equilibrium is simulated at the bottom while the top surface is stress free to
 1287 model the topographic evolution. The model is 450 km wide and 100 km deep. Two
 1288 zones of 100 km of each side of the models are set with a geotherm corresponding to a
 1289 500 Myr old lithosphere. The center is set at 500 Myr, 100 Myr and 30 Myr depending
 1290 on the cases analyzed (see figure 10, 11 & 12). The crust is 35 km thick with a 7 km
 1291 thick gabbroic layer in the lower crust. In the brittle areas, the lithosphere is elastoplastic
 1292 with a Mohr-Coulomb yield criterion. Crustal and mantle density are 2800 kg.m⁻³ and
 1293 3300 kg.m⁻³ respectively. Power law creep parameters are: crust, quartz (exponent, n = 3,
 1294 Activation energy, Q = 2 10 J.mol⁻¹, pre-exponent, A = 5. 10² MPa⁻ⁿ.s⁻¹) and plagioclase (n
 1295 = 3.2, Q = 2.38 10⁵ J.mol⁻¹, A = 3.3 10⁻⁴ MPa⁻ⁿ.s⁻¹), gabbroic lower crust (n = 3.05, Q =
 1296 3.5 10⁵ J.mol⁻¹, A = 1.25 10⁻¹ MPa⁻ⁿ.s⁻¹), mantle, dry olivine (n = 3, Q = 5.2 10⁵ J.mol⁻¹, A
 1297 = 7. 10⁴ MPa⁻ⁿ.s⁻¹) (see Lavier and Manatschal (2006) and references therein for additional
 1298 details). b) The material is both frictional and cohesive (initially the friction coefficient,
 1299 μ is 0.6 and the cohesion, C is 44 MPa). Both cohesion and friction decrease locally as a
 1300 function of plastic strain (10%) to trigger the formation of shear bands (to μ = 0.3 and C =
 1301 4 MPa). Serpentinization occurs in the mantle for temperature < 600°C and depth < 10 km.
 1302 There we further decrease the friction coefficient to 0.4. c) Schematic decrease in
 1303 viscosity associated with the formation of a ductile shear zone. The viscosity decreases
 1304 from that of plagioclase to quartz when the total work is equal to 4.10⁶J and the
 1305 temperature is between 300°C and 400°C. This parameterization leads to the formation of
 1306 a mixed zone of weak ductile material mixed with strong brittle material (for additional
 1307 details see Lavier and Manatschal (2006)).
 1308

A- Evolution of the viscosity through time - Low temperature Moho (450°C).



B- Strain rate evolution through time - Low temperature Moho (450°C).

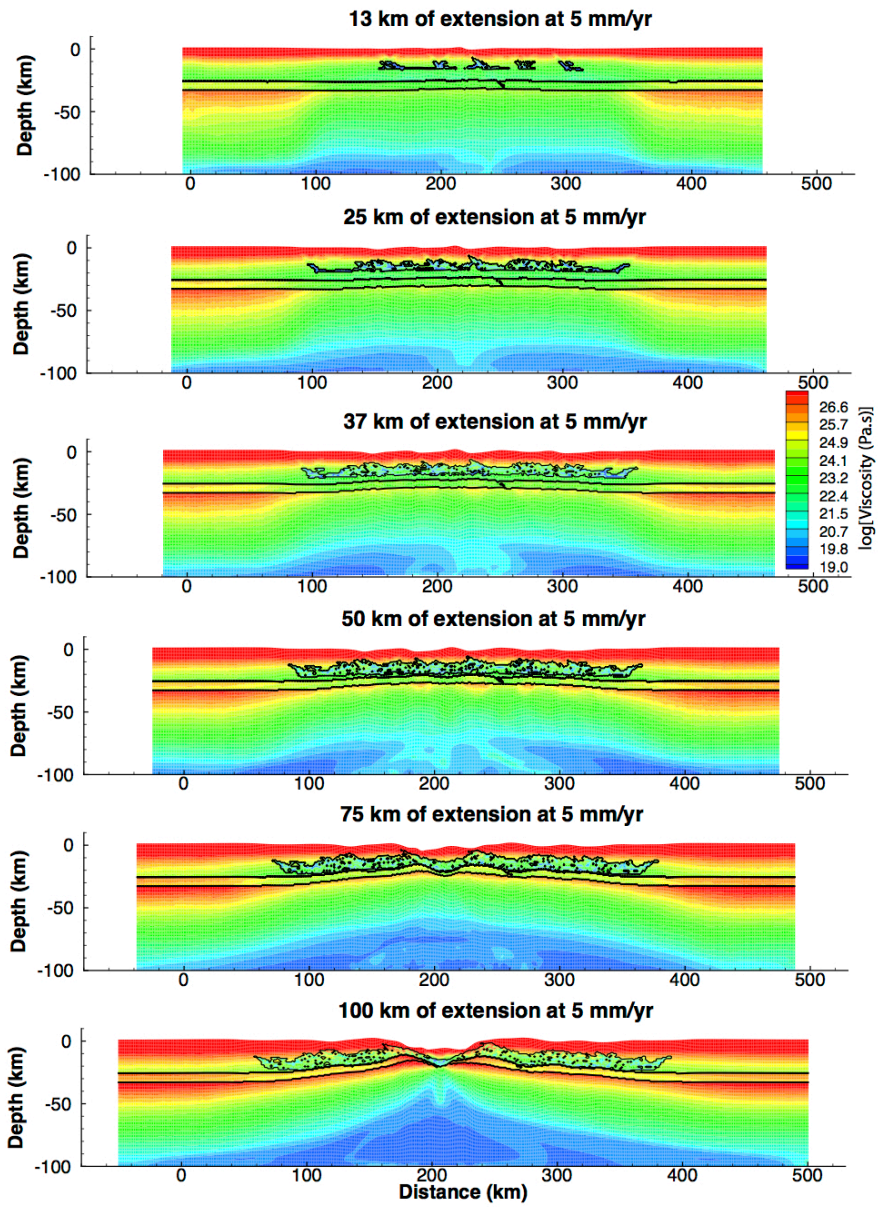


1310
1311
1312
1313
1314
1315
1316
1317
1318
1319

Fig. 10: The thermal structure is set such that the Moho temperature is 750°C and the bottom temperature is 1330°C. This situation is the case of a hot lithosphere corresponding to conditions similar to that past orogenic collapse. The lower and middle crusts are very weak and the mantle is mostly ductile. A) Evolution of the viscosity over 100 km or 20 Myr of extension. The lithosphere has a low average viscosity ($\sim 10^{23}$ Pa.s). The deformation is mostly viscous and crust and mantle deformation are decoupled for most of the evolution. Three small basins form and accommodated part of the extension in a brittle manner. As more extension is accommodated a shallow layer of hydrated middle crust forms and link the different basin. The crust and mantle thin uniformly while the

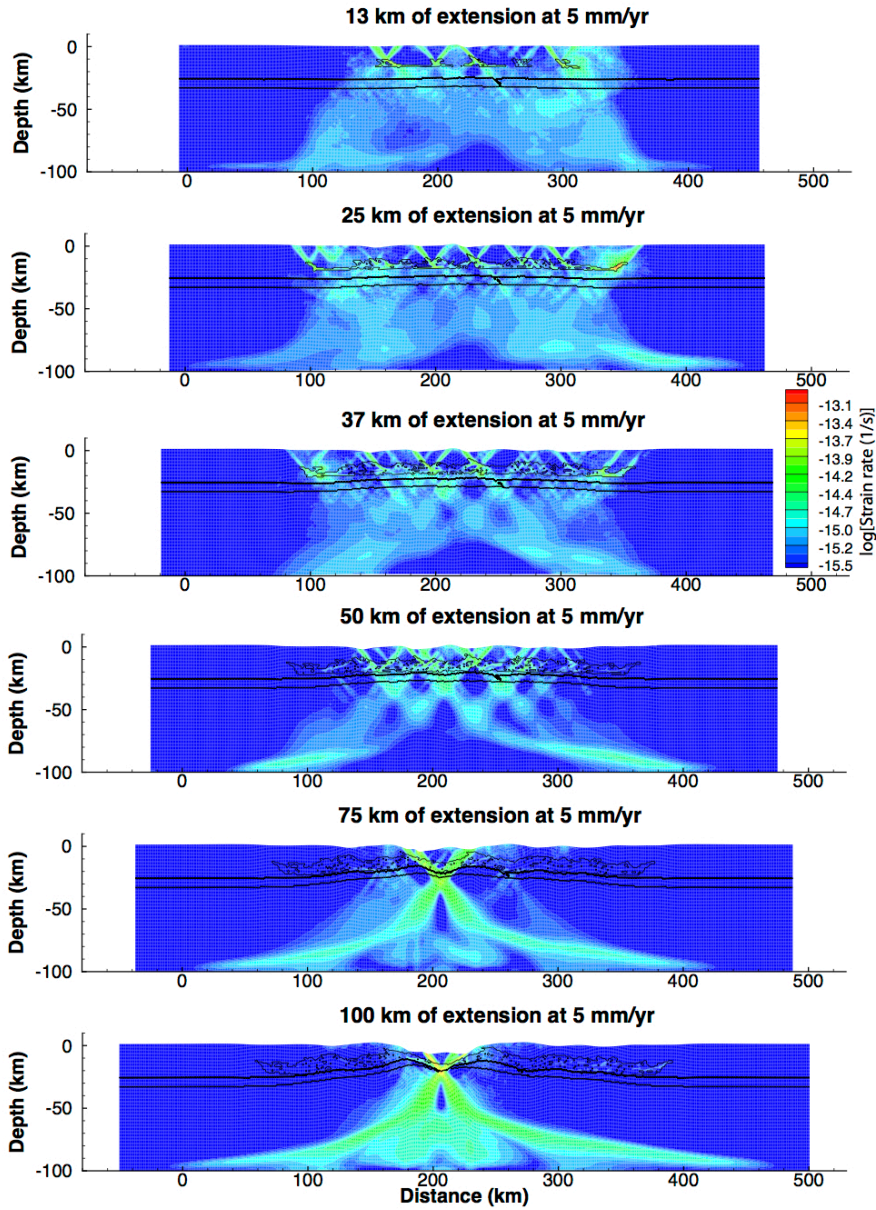
1320 middle crust is slowly exhumed close to the surface. After 75 km of extension the crust is
1321 uniformly thinned down to ~20 km. After 100 km, extension localizes in a very narrow
1322 basin or keystone block (near the distance 190 km), the deformation is still very
1323 distributed and the weak middle crust is exhumed on the flanks of the keystone. B) Until
1324 50 km of extension, the deformation is distributed in the middle to lower crust and mantle
1325 lithosphere with some normal faulting in the crust. After this period of ductile and
1326 distributed thinning, a large number of normal faults form across the zone of extension.
1327 This marks a period of embrittlement of the lithosphere that leads to the localization of the
1328 extension in one narrow keystone block (100 km) of extension.
1329

A- Evolution of the viscosity through time - Medium temperature Moho (600°C).



1330

B- Strain rate evolution through time - Medium temperature Moho (600°C).

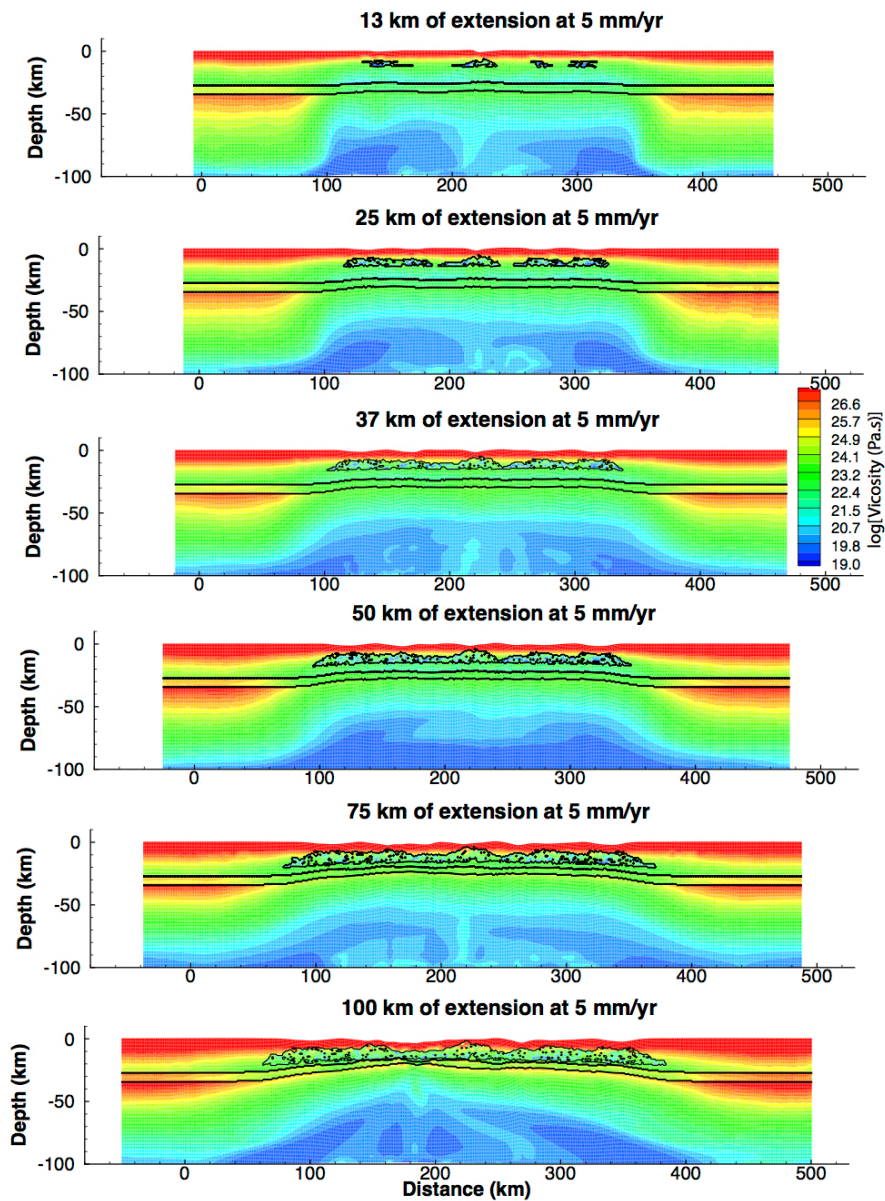


1331
1332
1333
1334
1335
1336
1337
1338
1339
1340

Fig. 11: The thermal structure is set such that the Moho temperature is 600°C and the bottom temperature is 1330°C. This situation is the case of a hot lithosphere corresponding to conditions of a young basin (100 Myr past orogenic collapse). A) Evolution of the viscosity over 100 km or 20 Myr of extension at 5 mm.yr⁻¹. In that case a keystone block H forms between 50 and 75 km of extension. This follows a period of pure shear distributed extension in the upper crust accompanied by the formation of mid-crustal layer of hydrated crust. The deformation in the crust and the mantle is decoupled until the keystone forms. The keystone is narrower (~40 km wide) than in the previous case. After 100 km of extension the crust is thinned to < 100 km and the mantle

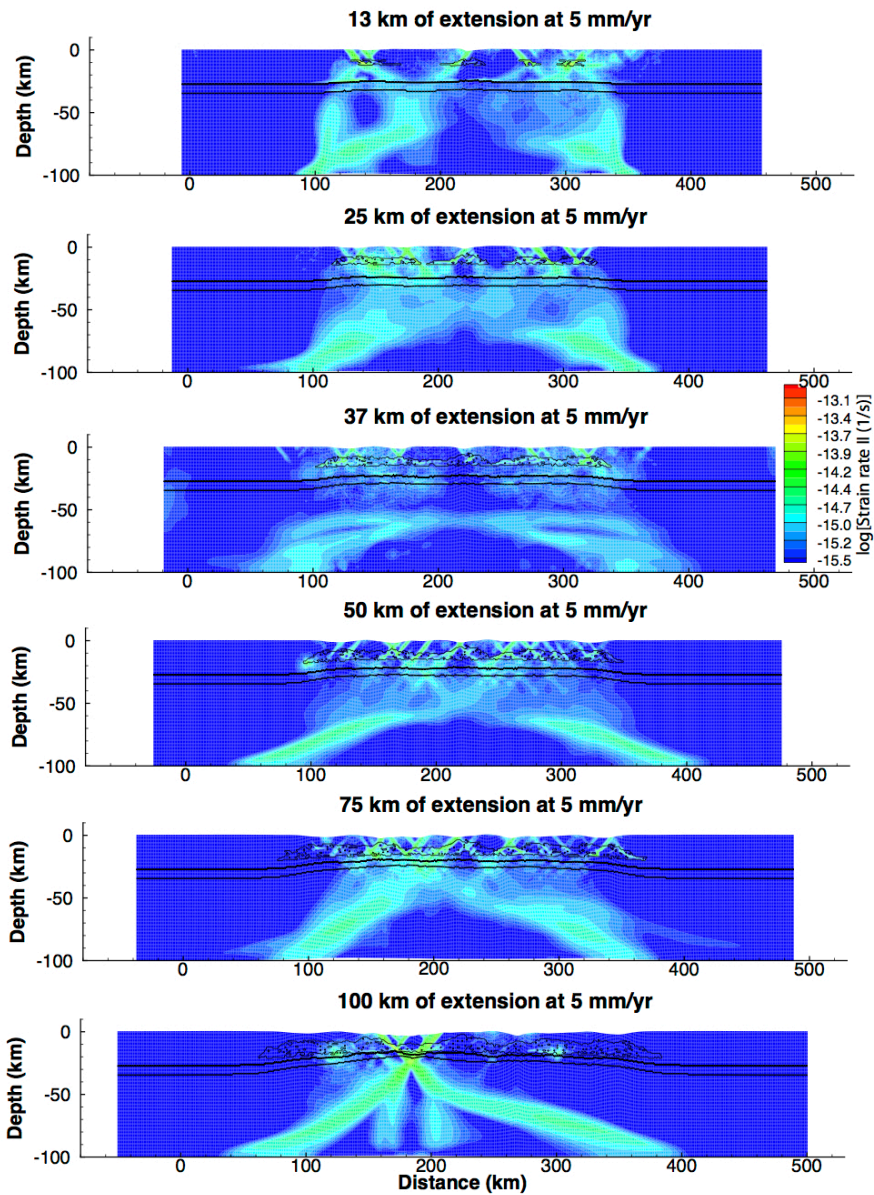
1341 lithosphere upwelling in a narrow channel below the crust. B) Deformation is distributed
1342 in the upper crust from the onset of deformation suggesting that a large proportion of the
1343 lithosphere can behave in a brittle manner. After 25 km of extension multiple half grabens
1344 have formed in the upper and the mantle lithosphere starts to deform in a brittle manner
1345 along multiple normal shear zone. After 50 km of extension the deformation zone
1346 narrows until it localizes in a keystone block (75 km of extension). Between 75 and 100
1347 km of extension the crust and lithosphere thin in the keystone block (see previous case).
1348

A- Evolution of the viscosity through time - High temperature Moho (750°C).



1349

B- Strain rate evolution through time - High temperature Moho (750°C).

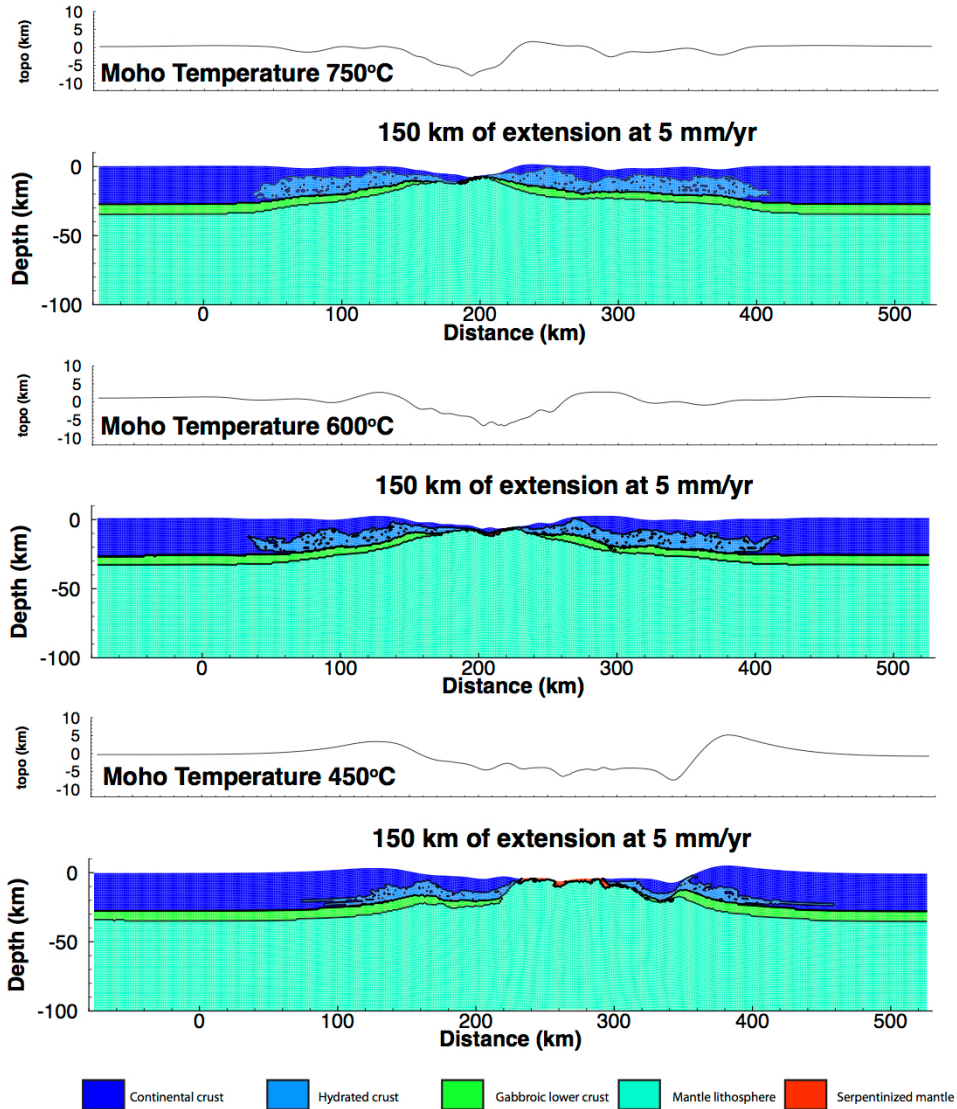


1350
1351
1352
1353
1354
1355
1356
1357
1358
1359

Fig. 12: The thermal structure is set such that the Moho temperature is 450°C and the bottom temperature is 1330°C. This situation is the case of a cold lithosphere. These are conditions in a very old orogeny (500 Myr) and a very strong lithosphere. The lower and middle crusts are very strong and brittle and the mantle lithosphere is brittle down to 50 km. A) Evolution of the viscosity over 100 km or 20 Myr of extension at 5 mm.yr⁻¹. The models show localization of the deformation in a 90 km wide keystone (initial block H) that evolves in a very localized and narrow set of conjugate margins (100 km of extension). Zones of weak hydrated crust (outlined in with black lines in the middle crust) form at the base of the brittle shear zone in the crust. The rift flanks are very developed

1360 (~5 km high) as well as the depth of the basin (~ 5 km). This situation is simulating an
1361 extreme case of thinning phase of the lithosphere. The crust thins from 35 km to almost 0
1362 km in 75 km of extension. This is unlikely to happen since the force needed to develop
1363 such a rift is $> 10^{13}$ N.m⁻¹. Additional weakening from magmatic processes is needed
1364 (Buck, 2005). B) Evolution of the second invariant of the strain rate that represents the
1365 effective shear strain rate and instantaneous deformation. From the beginning the
1366 deformation is localized on a few brittle fault zones and is coupled between the crust and
1367 mantle lithosphere. After 37 km of extension the deformation migrates inside the initial
1368 keystone block. After 75 km the deformation localizes into a major rolling-hinge that
1369 exhumes the mantle lithosphere at the bottom of a basin. This may correspond to the
1370 exhumation phase (Lavier and Manatschal, 2006).
1371

Final evolution (750°C-600°C-450°C)



1372
1373
1374
1375
1376
1377
1378
1379
1380
1381
1382
1383

Fig. 13: Final structure and topography of the lithosphere for each case after 150 km of extension. In all cases a localized thinned zone of crust forms. In the coldest case (Moho at 450°C) the final basin is wide (~230 km) with a large zone of exhumed serpentinized mantle and a very pronounced topography (max ~10 km). For the hottest case (Moho at 750°C) the basin is narrower (<100 km) and the topography is very asymmetric. The margin has developed a very clear upper-lower plate structure. Moreover the hydrated middle crust is exhumed close to the surface. Finally the medium case (Moho at 600°C) is akin to that of the Lavier and Manatschal (2006) case. The basin is asymmetric and some exhumation has occurred and the basin width is intermediate after the thinning phase (~160 km).

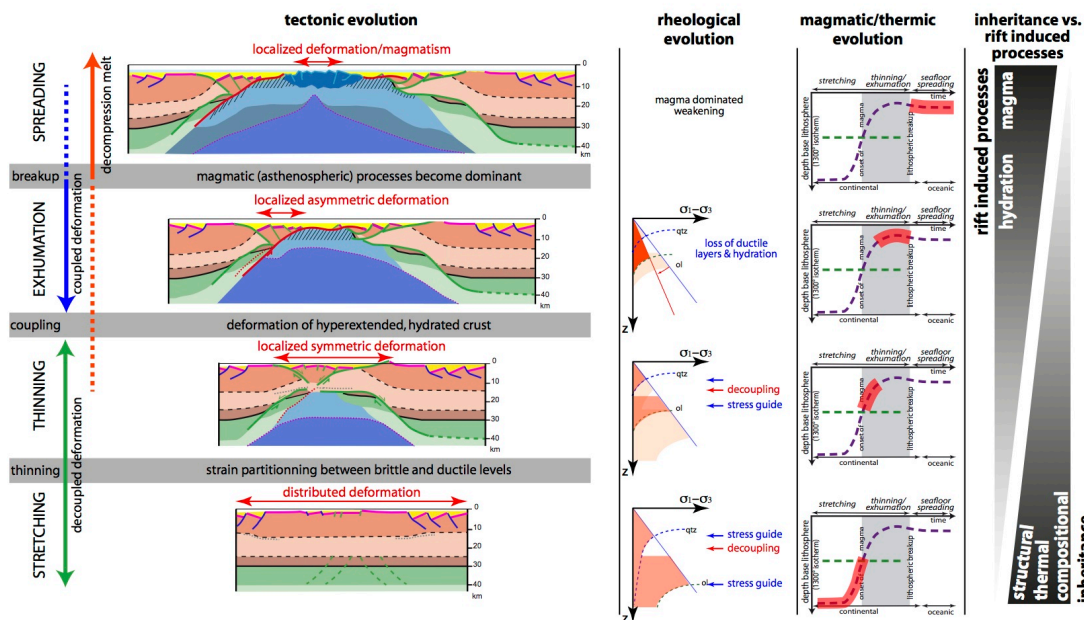


Fig. 14

Fig. 14: Conceptual model showing the tectonic, rheological and magmatic and thermal evolution of a magma-poor rifted margins and its relation to inheritance and rift induced processes.

References

Alves, L.S., 2011. Contribution from potential field methods to regional tectonic studies of the Western Iberian Continental Margin. *B. Geociencia Petrobras*, Rio de Janeiro, v. 19, n.1/2, p. 53-68

Arenas, R., Martínez Catalán, J.R., Sánchez Martínez, S., Díaz García, F., Abati, J., Fernández-Suárez, J., Andonaegui, P., Gómez-Barreiro, J., 2007. Paleozoic ophiolites in the Variscan suture of Galicia (northwest Spain): Distribution, characteristics, and meaning, in: Hatcher, R.D.J., Carlson, M.P., McBride, J.H., Martínez Catalán, J.R. (Eds.), *4-D Framework of Continental Crust*. Geological Society of America Memoir 200, pp. 1–20.

Barrier, E., Chamot-Rooke, N., Giordano, G., 2004, Geodynamic map of the Mediterranean. Commission for the Geological Map of the World, CCGM.

Bassi, G., Keen, C.E., Potter, P., 1993. Contrasting styles of rifting: Models and examples from the Eastern Canadian Margin. *Tectonics* 12, 639–655.

Bellahsen, N., Jolivet, L., Lacombe, O., Bellanger, M., Boutoux, A., Garcia, S., Mouthereau, F., Le Pourhiet, L., Gumiaux, C., 2012. Mechanisms of margin inversion in the external Western Alps: Implications for crustal rheology. *Tectonophysics* 560, 62–83.

Behn, M.D., Lin, J., 2000. Segmentation in gravity and magnetic anomalies along the U.S. East Coast passive margin: Implications for incipient structure of the oceanic lithosphere. *Journal of Geophysical Research* 105, 25769.

- 1411 Bertotti, G., Picotti, V., Bernoulli, D., Castellarin, A., 1993. From rifting to drifting:
 1412 tectonic evolution of the South-Alpine upper crust from the Triassic to the Early
 1413 Cretaceous. *Sedimentary Geology* 86, 53–76.
- 1414 Biteau, J.-J., Le Marrec, A., Le Vot, M., Masset, J.-M., 2006. The Aquitaine Basin.
 1415 *Petroleum Geoscience* 12, 247–273.
- 1416 Blaich, O.A., Tsikalas, F., Faleide, J.I., 2008. Northeastern Brazilian margin: Regional
 1417 tectonic evolution based on integrated analysis of seismic reflection and potential
 1418 field data and modelling. *Tectonophysics* In Press, Corrected Proof.
- 1419 Boillot, G., Winterer, E.L., 1988. Drilling on the Galicia margin: retrospect and prospect,
 1420 in: Boillot, G., Winterer, E.L., al., et (Eds.), *Proceedings of the Ocean Drilling*
 1421 *Program, Scientific Results*. College Station, TX (Ocean Drilling Program), pp.
 1422 809–828, doi:10.2973/odp.proc.sr.103.180.1988.
- 1423 Bois, C., Pinet, B., Roure, F., 1989. Dating lower crustal features in France and adjacent
 1424 areas from deep seismic profiles. *IUGG Monograph* 17–31.
- 1425 Bonatti, E., Ligi, M., Gasperini, L., Peyve, A., Raznitsin, Y., Chen, Y.J., (1994).
 1426 Transform migration and vertical tectonics at the Romanche Fracture Zone,
 1427 equatorial Atlantic, *Journal of Geophysical Research*, 99 (B11), pp. 21,779–21,802.
- 1428 Bronner, A., Sauter, D., Manatschal, G., Péron-Pinvidic, G., Munsch, M., 2011.
 1429 Magmatic breakup as an explanation for magnetic anomalies at magma-poor rifted
 1430 margins. *Nature Geoscience* 4, 549–553.
- 1431 Brun, J.P., Beslier, M.O., 1996. Mantle exhumation at passive margins. *Earth and*
 1432 *Planetary Science Letters* 142, 161–173.
- 1433 Buck, W.R., 1991. Modes of continental lithospheric extension. *Journal of Geophysical*
 1434 *Research Solid Earth* 96, 20161–20178.
- 1435 Buck, W.R., Lavier, L.L., Poliakov, A.N.B., 2005. Modes of faulting at mid-ocean ridges.
 1436 *Nature* 434, 719–23.
- 1437 Burg, J.-P., Driessche, Van den, J., Brun, J.-P., 1994. Syn- to post-thickening extension:
 1438 mode and consequences. *Comptes rendus l'Académie des Sciences Série 2.*
 1439 *Sciences de la terre des planètes* 319, 1019–1032.
- 1440 Butler, R.W.H., Tavarnelli, E., Grasso, M., 2006. Structural inheritance in mountain belts:
 1441 An Alpine–Apennine perspective. *Journal of Structural Geology* 28, 1893–1908.
- 1442 Canérot, J., 1989. Rifting eocrétacé et halocinèse sur la marge ibérique des Pyrénées
 1443 Occidentale (France). *Conséquences structurales*, Bulletin des centre de recherches
 1444 exploration-production Elf-Aquitaine, 13, p. 87–99.
- 1445 Chenin, P., Beaumont, C., 2013. Influence of offset weak zones on the development of
 1446 rift basins: activation and abandonment during continental extension and breakup.
 1447 *Journal of Geophysical Research Solid Earth* 1698–1720.
- 1448 Cowie, L. & Kusznir, N., 2012. Gravity inversion mapping of crustal thickness and
 1449 lithosphere thinning for eastern Mediterranean. *The leading edge*, pp.810–814.
- 1450 Dean, S.M., Minshull, T.A., Whitmarsh, R.B., Loudon, K.E., 2000. Deep structure of the
 1451 ocean-continent transition in the southern Iberia Abyssal Plain from seismic
 1452 refraction profiles: The IAM-9 transect at 40°20'N. *Journal of Geophysical*
 1453 *Research* 105, 5859–5885.
- 1454 Dick, H.J., Natland, J.H., 1996. Late-stage melt evolution and transport in the shallow
 1455 mantle beneath the East Pacific Rise, in: Mével, C., Gillis, K.M., Allan, J.F., Meyer,
 1456 P. (Eds.), *Proceeding of the Ocean Drilling Program, Scientific Results*, 147.
 1457 College Station, TX (Ocean Drilling Program), pp. 103–134.
- 1458 Direen, N.G., Stagg, H.M.J., Symonds, P.A., Colwell, J.B., 2008. Architecture of volcanic
 1459 rifted margins: new insights from the Exmouth – Gascoyne margin, Western
 1460 Australia. *Australian Journal of Earth Sciences* 55, 341–363.

- 1461 Dunbar, J.A., Sawyer, D.S., 1989. How preexisting weaknesses control the style of
1462 continental breakup. *Journal of Geophysical Research* 94 (B6), 7278-7292.
- 1463 Eldholm, O., Thiede, J., Taylor, E., 1989. Proceedings of the Ocean Drilling Program,
1464 Scientific Results, vol. 104. Ocean Drilling Program, College Station, TX, pp. 1033-
1465 1065.
- 1466 Féménias, O., Coussaert, N., Bingen, B., Whitehouse, M., Mercier, J.-C.C., Demaiffe, D.,
1467 2003. A Permian underplating event in late- to post-orogenic tectonic setting.
1468 Evidence from the mafic-ultramafic layered xenoliths from Beaunit (French Massif
1469 Central). *Chemical Geology* 199, 293–315.
- 1470 Franke, D., 2013. Rifting, lithosphere breakup and volcanism: Comparison of magma-
1471 poor and volcanic rifted margins. *Marine and Petroleum Geology* 43, 63–87.
- 1472 Froitzheim, N., Eberli, G.P., 1990. Extensional detachment faulting in the evolution of a
1473 Tethys passive continental margin, Eastern Alps, Switzerland. *Geological Society
1474 of America Bulletin* 102, 1297–1308.
- 1475 Froitzheim, N., Plašienka, D., Schuster, R., 2008. Alpine tectonics of the Alps and
1476 Western Carpathians, in: McCann, T. (Ed.), *The Geology of Central Europe:
1477 Volume 2: Mesozoic and Cenozoic*. The Geological Society, London, pp. 1141–
1478 1232.
- 1479 Galli, A., Le Bayon, B., Schmidt, M.W., Burg, J.-P., Caddick, M.J., Reusser, E., 2011.
1480 Granulites and charnockites of the Gruf Complex: Evidence for Permian ultra-high
1481 temperature metamorphism in the Central Alps. *Lithos* 124, 17–45.
- 1482 Gerya, T., 2012. Origin and models of oceanic transform faults. *Tectonophysics* 522, 34–
1483 54.
- 1484 Gerya, T.V., 2013. Initiation of Transform Faults at Rifted Continental Margins: 3D
1485 Petrological and Thermomechanical Modelling and Comparison to the Woodlark
1486 Basin. *Petrology* 21, 550–560.
- 1487 Gutiérrez-Alonso, G., Johnson, S.T., Weil, A.B., Pastor-Galán, D., Fernández-suárez, J.,
1488 2012. Buckling an orogen: The Cantabrian Orocline. *GSA Today* 22, 4–9.
- 1489 Hansmann, W., Müntener, O., Hermann, J., 2001. U-Pb zircon geochronology of a
1490 tholeiitic intrusion and associated migmatites at a continental crust-mantle
1491 transition, Val Malenco, Italy. *Schweizerische Mineralogische und Petrographische
1492 Mitteilungen* 80, 239–255.
- 1493 Hermann, J., Müntener, O., Trommsdorff, V., Hansmann, W., Piccardo, G.B., 1997.
1494 Fossil crust-to-mantle transition, Val Malenco (Italian Alps). *Journal of
1495 Geophysical Research* 102 (B9), 20123–20132.
- 1496 Higgins, A.K., Leslie, A.G., 2000. Restoring thrusting in the East Greenland Caledonides.
1497 *Geology* 28, 1019–1022.
- 1498 Huismans, R.S., Beaumont, C., 2007. Roles of lithospheric strain softening and
1499 heterogeneity in determining the geometry of rifts and continental margins.
1500 *Geological Society London Special Publications* 282, 111–138.
- 1501 Jammes, S., Lavier, L., Manatschal, G., 2010(a). Extreme crustal thinning in the Bay of
1502 Biscay and the Western Pyrenees: From observations to modelling.
1503 *Geochemistry, Geophysics, Geosystems* 11.
- 1504 Jammes, S., Manatschal, G., Lavier, L., 2010(b). Interaction between prerift salt and
1505 detachment faulting in hyperextended rift systems: The example of the Parentis and
1506 Mauléon basins (Bay of Biscay and western Pyrenees). *American Association of
1507 Petroleum Geologists Bulletin*, 94 (7), pp. 957-975.
- 1508 Jammes, S., Tiberi, C., Manatschal, G., 2010. 3D architecture of a complex transcurrent
1509 rift system: The example of the Bay of Biscay-Western Pyrenees. *Tectonophysics*,
1510 489 (1-4), pp. 210-226.

- 1511 Keen, C.E., Dickie, K., Dehler, S. a., 2012. The volcanic margins of the northern
1512 Labrador Sea: Insights to the rifting process. *Tectonics* 31.
- 1513 Lagabrielle, Y., 2009. Les Pyrénées, un analogue de marge distale à manteau exhumé ?
1514 Lagabrielle, Y., Labaume, P., de Saint Blanquat, M., 2010. Mantle exhumation, crustal
1515 denudation, and gravity tectonics during Cretaceous rifting in the Pyrenean realm
1516 (SW Europe): Insights from the geological setting of the lherzolite bodies.
1517 *Tectonics* 29 (4), n/a–n/a.
- 1518 Larsen, H.C., Saunders, A.D., 1998. Tectonism and volcanism at the southeast greenland
1519 rifted margin: A record of plume impact and later continental rupture, in: Saunders,
1520 A.D., Larsen, H.C., Clift, P.D., Wise, S.W.J. (Eds.), *Proceedings of the Ocean
1521 Drilling Program, Scientific Results*, 152. pp. 503–533.
- 1522 Larsen, H. C., et al. 1999. *Proceedings of the Ocean Drilling Program, Scientific Results*,
1523 vol. 163, Ocean Drilling Program, College Station, Texas, 1999.
- 1524 Lavier, L.L., Manatschal, G., 2006. A mechanism to thin the continental lithosphere at
1525 magma-poor margins. *Nature* 440, 324–328.
- 1526 Le Roux, V., Bodinier, J.-L., Tommasi, A., Alard, O., Dautria, J.-M., Vauchez, A.,
1527 Riches, A.J.V., 2007. The Lherz spinel lherzolite: Refertilized rather than pristine
1528 mantle. *Earth and Planetary Science Letters* 259, 599–612.
- 1529 Lister, G.S., Etheridge, M.A., Symonds, P.A., 1986. Detachment faulting and the
1530 evolution of passive continental margins. *Geology* 14, 246–250.
- 1531 Lister, G.S., Davis, G.A., 1989. The origin of metamorphic core complexes and
1532 detachment faults formed during Tertiary continental extension in the northern
1533 Colorado River region, U.S.A. *Journal of Structural Geology* 11, 65–94.
- 1534 Lundin, E.R., Doré, A.G., 2011. Hyperextension, serpentinization, and weakening: A new
1535 paradigm for rifted margin compressional deformation. *Geology* 39, 347–350.
- 1536 Manatschal, G. and Nievergelt, P., 1997. A continent-Ocean transition recorded in the Err
1537 and Platta nappes (Eastern Switzerland). *Eclogae Geologicae Helveticae*, 90, 3-28.
- 1538 Manatschal, G. and Bernoulli, D., 1998. Rifting and early evolution of ancient ocean
1539 basins, the record of the Mesozoic Tethys and the Galicia-Newfoundland margins.
1540 *Marine Geophysical Research*, 20, 371-381.
- 1541 Manatschal, G., 2004. New models for evolution of magma-poor rifted margins based on
1542 a review of data and concepts from West Iberia and the Alps. *International Journal
1543 of Earth Sciences* 93, 432–466.
- 1544 Manatschal, G., Müntener, O., 2009. A type sequence across an ancient magma-poor
1545 ocean continent transition: the example of the western Alpine Tethys ophiolites.
1546 *Tectonophysics* 473, 4–19.
- 1547 Martínez Catalán, J.R., 2011. Are the oroclines of the Variscan belt related to late
1548 Variscan strike-slip tectonics? *Terra Nova* 23, 241–247.
- 1549 Martínez Catalán, J.R., 2012. The Central Iberian arc, an orocline centered in the Iberian
1550 Massif and some implications for the Variscan belt. *International Journal of Earth
1551 Sciences* 101, 1299–1314.
- 1552 Masini, E., Manatschal, G., Mohn, G., Unternehr, P., 2012. Anatomy and tectono-
1553 sedimentary evolution of a rift-related detachment system: The example of the Err
1554 detachment (central Alps, SE Switzerland). *Bulletin of the Geological Society of
1555 America*, 124 (9-10), pp. 1535-1551.
- 1556 Masini, E., Manatschal, G., Mohn, G., 2013. The Alpine Tethys rifted margins:
1557 Reconciling old and new ideas to understand the stratigraphic architecture of
1558 magma-poor rifted margins. *Sedimentology* 60, 174–196.
- 1559 Mathieu, C., 1986. Geological history of the Parentis sub-Basin. *Bulletin du Centre de
1560 Recherches de Pau* 10, 33–47.

- 1561 McKenzie, D., 1978. Some remarks on the development of sedimentary basins. *Earth and*
1562 *Planetary Science Letters* 40, 25–42.
- 1563 Mohn, G., Manatschal, G., Müntener, O., Beltrando, M. and Masini, E., 2010.
1564 Unravelling the interaction between tectonic and sedimentary processes during
1565 lithospheric thinning in the Alpine Tethys Margins. *International Journal of Earth*
1566 *Sciences*, 99 supplement 1, 75-101.
- 1567 Mohn, G., Manatschal, G., Beltrando, M., Masini, E., Kuszniir, N., 2012. Necking of
1568 continental crust in magma-poor rifted margins: Evidence from the fossil Alpine
1569 Tethys margins. *Tectonics*, 31 (1), art. no. TC1012,
- 1570 Montanini, A., Tribuzio, R., Thirlwall, M., 2012. Garnet clinopyroxenite layers from the
1571 mantle sequences of the Northern Apennine ophiolites (Italy): Evidence for
1572 recycling of crustal material. *Earth and Planetary Science Letters* 351-352, 171–
1573 181.
- 1574 Mosar, J., 2003. Scandinavia's North Atlantic passive margin. *Journal of Geophysical*
1575 *Research*, 108(B8).
- 1576 Müntener, O., Hermann, J. and Trommsdorff V., 2000. Cooling history and exhumation
1577 of lower-crustal granulite and upper mantle (Malenco, Eastern Central Alps),
1578 *Journal of Petrology*, 41, 175-200.
- 1579 Müntener, O., Pettke, T., Desmurs, L., Meier, M., Schaltegger, U., 2004. Refertilization
1580 of mantle peridotite in embryonic ocean basins: trace element and Nd-isotopic
1581 evidence and implications for crust–mantle relationships, *Earth and Planetary*
1582 *Science Letters* 221, 293–308.
- 1583 Müntener, O., Manatschal, G., 2006. High degrees of melt extraction recorded by spinel
1584 harzburgite of the Newfoundland margin: The role of inheritance and consequences
1585 for the evolution of the southern North Atlantic. *Earth and Planetary Science Letters*
1586 252, 437–452.
- 1587 Müntener, O., Manatschal, G., Desmurs, L., Pettke, T., 2010. Plagioclase Peridotites in
1588 Ocean-Continent Transitions: Refertilized Mantle Domains Generated by Melt
1589 Stagnation in the Shallow Mantle Lithosphere. *Journal of Petrology* 51, 255–294.
- 1590 Montanini, A., Tribuzio, R., Thirlwall, M., 2012. Garnet clinopyroxenite layers from the
1591 mantle sequences of the Northern Apennine ophiolites (Italy): Evidence for
1592 recycling of crustal material. *Earth and Planetary Science Letters* 351-352, 171–
1593 181.
- 1594 Pastor-Galan, D., Gutierrez-Alonso, G., Zulauf, G., Zanella, F., 2012. Analogue
1595 modelling of lithospheric-scale orocline buckling: Constraints on the evolution of
1596 the Iberian-Armorican Arc. *Geological Society of America Bulletin* 124, 1293–
1597 1309.
- 1598 Peressini, G., Quick, J.E., Sinigoi, S., Hofmann, A.W., Fanning, M., 2007. Duration of a
1599 Large Mafic Intrusion and Heat Transfer in the Lower Crust: a SHRIMP U-Pb
1600 Zircon Study in the Ivrea-Verbano Zone (Western Alps, Italy). *Journal of Petrology*
1601 48, 1185–1218.
- 1602 Pérez-Gussinyé, M., Reston, T.J., 2001. Rheological evolution during extension at
1603 nonvolcanic rifted margins: Onset of serpentinization and development of
1604 detachments leading to continental breakup. *Journal of Geophysical Research* 106,
1605 3961–3975.
- 1606 Péron-Pinvidic, G., Manatschal, G., 2009. The final rifting evolution at deep magma-poor
1607 passive margins from Iberia-Newfoundland: a new point of view. *International*
1608 *Journal of Earth Sciences* 98, 1581–1597.
- 1609 Péron-Pinvidic, G., Manatschal, G., 2010. From microcontinents to extensional
1610 allochthons: witnesses of how continents rift and break apart? *Petroleum*

1611 Geoscience 16, 189–197.

1612 Peron-Pinvidic, G., Manatschal, G., Osmundsen, P.T., 2013. Structural comparison of
1613 archetypal Atlantic rifted margins: A review of observations and concepts. *Marine*
1614 *and Petroleum Geology* 43, 21–47.

1615 Piccardo, G.B., 2003. Mantle processes during ocean formation: Petrologic records in
1616 peridotites from the Alpine-Apennine ophiolites. *Episodes* 26.

1617 Piccardo, G.B., 2009. Geodynamic evolution of the Jurassic Ligurian Tethys viewed from
1618 the Mantle perspective. *Bollettino della Società Geologica Italiana* 128, 565–574.

1619 Piqué, A., Laville, E., 1996. The central Atlantic rifting: Reactivation of Palaeozoic
1620 structures? *Journal of Geodynamics* 21, 235–255.

1621 Rampone, E., Hofmann, A.W., 2012. A global overview of isotopic heterogeneities in the
1622 oceanic mantle. *Lithos* 148, 247–261.

1623 Reston, T., Manatschal, G. 2011. Rifted margins: Building blocks of later collision.
1624 *Frontiers in Earth Sciences*, 4, pp. 3-21.

1625 Ring, U., 1994. The influence of preexisting structure on the evolution of the Cenozoic
1626 Malawi rift (East African rift system). *Tectonics* 13, 313–326.

1627 Robertson, A.H.F. et al., 2013. Tectonic development of the Vardar ocean and its
1628 margins: Evidence from the Republic of Macedonia and Greek Macedonia.
1629 *Tectonophysics*, 595-596, pp.25–54.

1630 Rossi, P., Cocherie, A., Fanning, C.M., Deloule, É., 2006. Variscan to eo-Alpine events
1631 recorded in European lower-crust zircons sampled from the French Massif Central
1632 and Corsica, France. *Lithos* 87, 235–260.

1633 Ryan, W. B. F., Carbotte, S.M., Coplan, J., O'Hara, S., Melkonian, A., Arko, R., Weissel,
1634 R.A., Ferrini, V., Goodwillie, A., Nitsche, F., Bonczkowski, J., Zemsky, R., 2009.
1635 Global Multi-Resolution Topography (GMRT) synthesis. *Geochemistry,*
1636 *Geophysics, Geosystems*, 10 (3)

1637 Schmid, S.M. et al., 2004. Tectonic map and overall architecture of the Alpine orogen.
1638 *Eclogae Geologicae Helvetiae*, 97, pp.93–117.

1639 Schuster, R., Stüwe, K., 2008. Permian metamorphic event in the Alps. *Geology* 36, 603.

1640 Serrano, O., Delmas, J., Hanot, F., Vially, R., Herbin, J. P., Houel, P., Tourlière, B., 2006.
1641 Le bassin d'Aquitaine: valorisation des données sismiques, cartographie structurale
1642 et potentiel pétrolier, B.R.G.M ed.

1643 Stojadinovic, U. et al., 2013. The balance between orogenic building and subsequent
1644 extension during the Tertiary evolution of the NE Dinarides: Constraints from low-
1645 temperature thermochronology. *Global and Planetary Change*, 103, pp.19–38.
1646 Available at: <http://linkinghub.elsevier.com/retrieve/pii/S0921818112001610>
1647 [Accessed November 22, 2013].

1648 Sutra, E., Manatschal, G., 2012. How does the continental crust thin in a hyperextended
1649 rifted margin? Insights from the Iberia margin. *Geology*, 40 (2), 139–142.

1650 Sutra, E., Manatschal, G., Mohn, G., Unternehr, P., 2013. Quantification and restoration
1651 of extensional deformation along the Western Iberia and Newfoundland rifted
1652 margins. *Geochemistry, Geophysics, Geosystems* 14, 2575–2597.

1653 Taylor, B., Goodliffe, A., Martinez, F., 2009. Initiation of transform faults at rifted
1654 continental margins. *Comptes Rendus Geosci.* 341, 428–438.

1655 Thiébaud, J., M. Debeaux, C. Durand-Wackenheim, P. Souquet, Y. Gourinard, Y. Bandet
1656 and M. J. Fondécave-Wallez, 1988. Métamorphisme et halocinèse créacés dans les
1657 évaporites de Betchat le long du Chevauchement Frontal Nord-Pyrénéen (Haute
1658 Garonne et Ariège, France), *Comptes rendus de l'Academie des sciences, Paris*, 307,
1659 p. 1535-1540.

- 1660 Thiébaud, J., C. Durand-Wackenheim, M. Debeaux and P. Souquet, 1992.
1661 Métamorphisme des évaporites triasiques du versant nord des Pyrénées centrales et
1662 occidentales, *Bulletin de la Société d'histoire Naturelle*, 128, p. 77-84.
- 1663 Tommasi, A., Vauchez, A., 2001. Continental rifting parallel to ancient collisional belts:
1664 an effect of the mechanical anisotropy of the lithospheric mantle. *Earth and*
1665 *Planetary Science Letters* 185, 199–210.
- 1666 Tribuzio, R., Thirlwall, M.F., Messiga, B., 1999. Petrology, mineral and isotope
1667 geochemistry of the Sondalo gabbroic complex (Central Alps, Northern Italy):
1668 implications for the origin of post-Variscan magmatism. *Contributions to*
1669 *Mineralogy and Petrology* 136, 48–62.
- 1670 Tsikalas, F., Faleide, J.I., Kusznir, N.J., (2008). Along-strike variations in rifted margin
1671 crustal architecture and lithosphere thinning between northern Vøring and Lofoten
1672 margin segments off mid-Norway. *Tectonophysics*, 458 (1-4), pp. 68-81.
- 1673 Tucholke, B.E., Sawyer, D.S., Sibuet, J.C., 2007. Breakup of the Newfoundland-Iberia
1674 rift. *Geological Society London Special Publications* 282, 9–46.
- 1675 Tucholke, B.E., Sibuet, J.-C., 2007. Leg 210 synthesis: tectonic, magmatic, and
1676 sedimentary evolution of the Newfoundland-Iberia rift: a synthesis based on ocean
1677 drilling through ODP Leg 210, in: Tucholke, B.E., Sibuet, J.-C., Klaus, A. (Eds.),
1678 *Proceedings of Ocean Drilling Program - Scientific Results*, 210, pp. 1–56.
- 1679 Tugend, J., Manatschal, G., Kusznir, N.J., Masini, E., Mohn, G., Thinon, I., 2014
1680 Formation and deformation of hyperextended rift systems: insights from rift domain
1681 mapping in the Bay of Biscay - Pyrenees (submitted to *Tectonics*).
- 1682 Von Raumer, J.F., Bussy, F., Schaltegger, U., Schulz, B., Stampfli, G.M., 2012. Pre-
1683 Mesozoic Alpine basements--Their place in the European Paleozoic framework.
1684 *Geological Society of America Bulletin* 125, 89–108.
- 1685 Welford, J.K., Shannon, P.M., O'Reilly, B.M., Hall, J., 2012. Comparison of lithosphere
1686 structure across the Orphan Basin-Flemish Cap and Irish Atlantic conjugate
1687 continental margins from constrained 3D gravity inversions. *Journal of the*
1688 *Geological Society* 169, 405–420.
- 1689 Wernicke, B., 1985. Uniform-sense normal simple shear of the continental lithosphere.
1690 *Canadian Journal of Earth Sciences* 22, 108–125.
- 1691 Whitmarsh, R.B., Sawyer, D.S., 1996. The ocean/continent transition beneath the Iberia
1692 Abyssal Plain and continental-rifting to seafloor-spreading processes. *Proceedings*
1693 *of the Ocean Drilling Program - Scientific Results* 149, 713–733.
- 1694 Whitmarsh, R.B., Wallace, P., 2001. The rift-to-drift development of the west Iberia
1695 nonvolcanic continental margin: a summary and review of the contribution of
1696 Ocean Drilling Program Leg 173, in: Beslier, M.-O., Whitmarsh, R.B., Wallace, P.J.,
1697 Girardeau, J. (Eds.), *Proc. ODP, Sci. Results*. p. Available from World Wide Web:
1698 <http://www-odp.tamu.edu/publications/173_SR/synth/synth.htm>.
- 1699 Wilson, R.C.L., Whitmarsh, R.B., Froitzheim, N., Taylor, B., 2001. Introduction: the land
1700 and sea approach. *Geological Society London Special Publications* 187, 1–8.
- 1701 Zelt, C.A., Sain, K., Naumenko, J.V., Sawyer, D.S., 2003. Assessment of crustal velocity
1702 models using seismic refraction and reflection tomography. *Geophys. J. Int.* 153,
1703 609–626.
- 1704 Ziegler, P. A. and Dèzes, P. (2006). Crustal Evolution of Western and Central Europe. In
1705 Gee, D. G. and Stephenson, R. A., editors, *European Lithosphere Dynamics*, pp.43–
1706 56. Geological Society, London, *Memoir* 32.
- 1707
1708
1709



1710
1711
1712
1713
1714
1715
1716
1717
1718
1719

Gianreto Manatschal is a Professor at the Institut de Physique du Globe at the University of Strasbourg. He received his PhD in geology from the ETH Zürich, Switzerland in 1995. After postdoctoral appointments at the Danish Lithosphere Centre and at ETH Zürich, he moved to Strasbourg (France), where he became full professor in tectonics in 2003. His major research interests are in the formation and reactivation of rifted margins in the Atlantic and Alpine Tethys domains.



1720
1721
1722
1723
1724
1725
1726
1727
1728
1729
1730
1731
1732

Luc Lavier is an associate Professor at the Department of Geological Sciences and at the Institute for Geophysics at the University of Texas at Austin. He received his PhD in geophysics from the Lamont-Doherty Earth Observatory at Columbia University, NY, in 2000. After postdoctoral appointments at the GeoForschungsZentrum Postdam, Germany and at the California Institute of Technology, he moved to Austin (Texas), where he started as associate research Scientist in 2003 and then became an assistant Professor in 2009. He became associate Professor in 2014. His research interests include understanding the rheological evolution of materials in order to better constrain the tectonic evolution of the Earth.



1733
1734

1735 Pauline Chenin is a PhD student at the Institut de Physique du Globe in Strasbourg
1736 (France). She studied tectonics and structural geology at University of Strasbourg
1737 and numerical modelling at the University of Grenoble (France). Her fields of
1738 interest include large-scale deformation processes and their relationships with pre-
1739 existing structures.
1740